

Greenhouse gasses emissions and their trends over the last three decades across Africa

Mounia Mostefaoui¹, Philippe Ciais², Matthew J. McGrath², Philippe Peylin², Prabir K. Patra³, Yolandi Ernst⁴

¹Laboratoire de Météorologie Dynamique/IPSL, École Normale Supérieure, PSL Research University, Sorbonne University, École Polytechnique, IP Paris, CNRS, Paris, France.

²Laboratoire des Sciences du Climat et de l'Environnement, 91190 Gif-sur-Yvette, France.

³Research Institute for Global Change, JAMSTEC, Yokohama 2360001, Japan.

⁴Global Change Institute, University of the Witwatersrand, Johannesburg, South Africa.

Correspondence to: mounia.mostefaoui@polytechnique.edu

Key words: greenhouse gasses, anthropogenic emissions and removals, fossil fuels, land-use, land-use change and forestry, Africa, bottom-up, top-down atmospheric inversions, UNFCCC inventories, Global Carbon Project, PRIMAP-hist, IPCC sectors, climate change, Paris Agreement, Global Stocktake, Monitoring, Reporting and Verification.

Abstract. A key goal of the Paris Agreement (PA) is to reach net-zero Greenhouse Gasses (GHG) emissions by 2050 globally, which requires mitigation efforts from all countries. Africa's rapidly growing population and GDP makes this continent important for GHG emission trends. In this paper, we study the emissions of carbon dioxide (CO₂), methane (CH₄) and nitrous oxide (N₂O) in Africa over three decades (1990-2018). We compare bottom-up (BU) approaches including UNFCCC national inventories, FAO, PRIMAP-hist, process-based ecosystem models for CO₂ fluxes in the Land Use, Land Use Change and Forestry (LULUCF) sector, and global atmospheric inversions. For inversions, we applied different methods to separate anthropogenic CH₄ emissions. The BU inventories show that over the decade 2010-2018, less than ten countries represented more than 75% of African fossil CO₂ emissions. With a mean of 1373 MtCO₂ yr⁻¹, total African fossil CO₂ emissions over 2010-2018 represent only 4% of global fossil emissions. Yet, these emissions grew by +34% from 1990-1999 to 2000-2009 and by +31% over 2000-2009 to 2010-2018, which represent more than a doubling in 30 years. This growth rate is more than twice faster than the global growth rate of fossil CO₂ emissions. The anthropogenic emissions of CH₄ grew by 5% from 1990-1999 to 2000-2009 and by 14.8% from 2000-2009 to 2010-2018. The N₂O emissions grew by 19.5% from 1990-1999 to 2000-2009; and by 20.8% from 2000-2009 to 2010-2018. When using the mean of estimates from UNFCCC reports (including the land use sector), with corrections from outliers, Africa was a mean source of greenhouse gasses of 2622^{3239}_{2186} MtCO₂e yr⁻¹ from all BU estimates (sub- and superscript indicating min-max range uncertainties), and of $+2637^{5873}_{1761}$ MtCO₂e yr⁻¹ from top-down (TD) methods, during their overlap period from 2001 to 2017. Although the mean values are consistent, the range of TD estimates is larger than the one of BU estimates, indicating that sparse atmospheric observations and transport model errors do not allow us to use inversions to reduce the uncertainty of BU estimates. A main source of uncertainty comes from CO₂ fluxes in the land-use sector (LULUCF) for which the spread across inversions is larger than 50%, especially in Central Africa. Moreover, estimates from national UNFCCC communications differ widely depending on whether the large sinks in a few countries are corrected to more plausible

39 values using more recent national sources following the methodology of Grassi et al. (2022). The median of CH₄
40 emissions from inversions based on satellite retrievals and surface station networks are consistent with each other
41 within 2% at continental scale. The inversion ensemble also provides consistent estimates of anthropogenic CH₄
42 emissions with BU inventories such as PRIMAP-hist. For N₂O, inversions systematically show higher emissions than
43 inventories, on average about 4.5 times more than PRIMAP-hist, either because natural N₂O sources cannot be
44 separated accurately from anthropogenic ones in inversions, or because BU estimates ignore indirect emissions and
45 under-estimate emission factors. Future improvements can be expected thanks to a denser network for monitoring
46 atmospheric concentrations. This study helps to introduce methods to enhance the scope of use of various published
47 datasets and allows to compute budgets thanks to recombinations of those data products. Our results allow to
48 understand uncertainty and trends of emissions and removals in a region of the world where few observations exist
49 and most inventories are based on default IPCC guidelines values. The results can therefore serve as a support tool for
50 the Global Stocktake (GST) of the Paris Agreement. The referenced datasets related to figures are available at:
51 <https://doi.org/10.5281/zenodo.7347077> (Mostefaoui et al., 2022).

52

Introduction

53 Large global reductions of greenhouse gasses (GHG) emissions are needed to avoid “dangerous
54 anthropogenic interference with the climate system” (IPCC, 2021). The Paris Agreement (PA) aims at
55 limiting global warming below 2°C and reaching “net-zero GHG emissions by 2050” (UNFCCC,
56 2015). To improve the monitoring of emissions trends, the PA has an Enhanced Transparency
57 Framework (ETF) by which countries will have to report their GHG emissions and removals under a
58 standardized format starting in 2024 (Perugini et al., 2021; UNFCCC, 2021) through Biennial
59 Transparency Reports (BTR), with the ambition to use up-to-date data and best available science to
60 improve national inventories. This represents a challenge for many developing countries, where
61 emissions inventories have been irregular.

62 Recent analyses predict a fast increase of African emissions correlated with demographic growth. The
63 African population is expected to double from 1.2 billion in 2019 to 2.5 billion at the 2050 horizon
64 (UN, 2019). Using the TIAM-ECN Integrated Assessment Model (IAM) developed with data from the
65 International Energy Agency (IEA), van der Zwaan et al., (2018) concluded that greenhouse gasses
66 (GHG) emissions from Africa will become substantial at the global scale by 2050. In Shared Socio-
67 economic Pathways (SSP) projection scenarios, Africa and the Middle East are grouped together
68 despite having very different geographies, per capita emissions and Gross Domestic Product (GDP)
69 (IIASA, 2017). According to IAM projections, the minimum projected share of Africa in global
70 emissions would be close to 10% by 2050 for a business-as-usual pathway. An “explosive growth in
71 African combustion emissions” (Lioussse et al., 2014) could not be excluded from 2030 to 2050, if no
72 drastic mitigation policies are implemented (IPCC, 2021). If a stringent emissions reduction pathway
73 limiting global warming to +2 °C is adopted, Africa could contribute to around 20% of global emissions
74 by 2050, becoming the second largest worldwide emitting region. Further, under stringent climate
75 policy scenarios, CH₄ and N₂O emissions in Africa were projected to contribute 80% of the total
76 emissions of these two gasses in 2050 (van der Zwaan et al., 2018). Therefore, Africa will become an
77 important global emission contributor under any mitigation pathway with a demographical and
78 industrial development increase.

79 There are 56 African countries represented in the United Nations. National emissions reports to the
80 United Nations Convention Framework on Climate Change (UNFCCC) are available for 53 countries,
81 including all major African emitters. Africa as a whole ranks fifth worldwide in terms of territorial
82 fossil fuels use with a total of 1449 MtCO_{2e}, in-between the Russian Federation and Japan
83 (Friedlingstein et al., 2020). The global share of Africa is ~ 4% of fossil CO₂ (FCO₂) emissions, ~ 16

84 % of CH₄ emissions (Saunois et al., 2020) and ~ 25% of N₂O emissions (Tian, 2020). South Africa is
85 the biggest FCO₂ emitter in the continent, and ranked twelve on the global scale, just after Brazil.

86 Despite projections of strong growth of emissions and population in Africa, the continent is under-
87 studied and lacks up-to-date comprehensive assessments of GHG emissions and removals, given
88 sporadic and often outdated reports by individual countries. The literature tends to be scarce about
89 African countries, and their emissions have rarely been analyzed comprehensively using the results
90 from both statistical inventories that are also referred to as bottom-up (BU) methods, and from top-
91 down (TD) atmospheric inversions. Country reports estimate GHG emissions through statistical
92 inventories using estimates of national sectoral activity data multiplied by emissions factors, with three
93 levels of refinements depending on countries, named Tier 1 for default emissions factors, Tier 2 for
94 country-specific emissions factors / activity data and Tier 3 for more emissions factors / activity with
95 tailored representation at the scale of process. Other BU inventories for assessing national emissions
96 also exist: they are based on the same approach as country-reported inventories but use their own
97 parameters for activity data and emissions factors coming from research groups, international statistical
98 agencies, etc. Process-based ecosystem models developed by the research community are not used by
99 countries. They are based on the representations of complex ecosystem processes and can also be
100 viewed as a BU method. Besides, another approach is named “top-down” and refers to atmospheric
101 inversions. Inversions consist in estimating causes (emissions and sinks) based on consequences
102 (concentrations). The inverse modeling approach consists in adjusting a priori fluxes to the atmospheric
103 transport in order to be as adjusted as possible with observation data by minimizing a cost function.
104 This is a mathematically complex problem under constrained because every point of the globe is an
105 unknown emission, and there is only a limited number of observations: “regularization” techniques are
106 used to find a unique solution. The African ground-based atmospheric network used by inversions is
107 very sparse. There are only three currently active surface flasks over this whole continent, located in
108 Namibia (Gobabeb), in the Seychelles (Mahe Island), and in South Africa (Cape Point). The one in
109 Algeria (Assekrem) was terminated on 26/08/2020, and the one in Kenya has been inactive since
110 21/06/2011. The characteristics of the surface flasks in Africa, available on the NOAA website are
111 summarized in Table S1. Inversion results are therefore uncertain due to this small number of
112 atmospheric stations over the continent (Nickless et al., 2020).

113 A previous analysis of African emissions was solely focused on FCO₂ emissions during the decade
114 2000-2009 (Canadell et al., 2009). A first budget for the period 1990-2009 was provided at the
115 continental scale with the RECCAP1 project (Valentini et al., 2014). Ayompe et al. (2020) studied
116 recent FCO₂ emissions trends, using International Energy Agency (IEA) data. Other studies are region-

117 specific or sector-specific, focusing exclusively on agriculture (Bombelli et al., 2009), on natural
118 ecosystems in Sub-Saharan Africa (Kim et al., 2016) or in individual countries such as Kenya (Zhu et
119 al., 2018).

120 Paying attention not only to commonly identified big emitters like South Africa, but also to medium
121 emitters and to emerging emitters is important, not only in terms of scientific assessment, but also for
122 financial and climate policy purposes under the PA. The Monitoring, Reporting and Verification
123 (MRV) provisions of the PA indeed require scientific and policy tools to verify the pledges made by
124 all the signatory countries. Instruments for financial transfers for mitigation and adaptation like the
125 Green Fund on Climate Change (GCF) and the REDD+ initiatives cover the African scope and will
126 require scientific assessment of trends for impact evaluation and credibility purposes, and as an
127 incentive for continued investments. As part of the Global Stock Take (GST) under article 14 of the
128 PA aiming at assessing “collective progress”, all signatory parties will have to show their contributions
129 to the global mitigation efforts. These efforts will be evaluated within a MRV system which includes
130 the requirement for developing countries to submit their Biennial Update Reports (BUR) on a biennial
131 basis starting in 2024. As no standard global reporting framework has been required to date, we
132 anticipate that the data available for the first stocktake in 2023 will be very heterogeneous. As a
133 continent gathering non-Annex I countries exclusively, the African case is featured by the scarcity of
134 national official inventories which have been provided to date on a voluntary basis through National
135 Communication (NC) and BUR. BU estimates of emissions established by independent scientific
136 methods are also discussed in the present study. In this context, different and complementary
137 observation-based methods assessing national GHG emissions and sinks are needed.

138 The aim of this paper is to evaluate relative merits of different existing types of datasets for the
139 assessment of African emissions and removals and their trends for CO₂, CH₄ and N₂O during the last
140 three decades. In this paper, we standardize the metrics and scope of application for different categories
141 of GHG emissions to discuss budgets. We also validate and benchmark different independent datasets
142 to evaluate the possibility to use them as a verifying tool for official country-reported data. In order to
143 cover all GHG sectors, we also describe recombinations of different historical datasets for the last 30
144 years that are necessary to fill the gap for some missing past sectoral emissions. This study offers a
145 comparison of data products originally combined to compute a budget and an evaluation of their
146 relative merits. The different data products discussed here include different BU approaches, including
147 official countries communications to the UNFCCC and estimations from the Food and Agriculture
148 Organization (FAO), Carbon Dioxide Information Analysis Center (CDIAC), global inventories for
149 anthropogenic emissions (PRIMAP-hist which integrates combinations of various datasets including

150 FAO and Global Carbon Project (GCP)), and process-based models for land CO₂ fluxes with 14
151 Dynamic General Vegetation Models (DGVM) from the TRENDY version 9 ensemble (Table 1). We
152 also analyze and combine TD products to discuss individual gas and to compute budgets: three
153 atmospheric global inversions for CO₂ land fluxes; 22 inversions for CH₄ emissions (11 inversion
154 models using surface station data and 11 satellite inversion models) and CH₄ wildfire emissions from
155 the Global Fires Emission Dataset (GFED) version 4. We used three inversion models for N₂O fluxes
156 (PyVAR model, TOMCAT-INVICAT model, and MIROC4-ACTM model (see Table 1). Inversions
157 only solve for total fluxes or at best for groups of sectors, whereas BU estimates have a larger number
158 of sectors. In Table 2, we present the correspondence between ‘sectors’ defined by the TD and BU
159 methods. For all datasets, we chose an atmospheric convention with negative values representing
160 removals from the atmosphere (i.e. land sink). We deliver an original comparison of BU estimates from
161 national inventories, global inventories, and process-based models, with TD estimates from
162 atmospheric inversions over Africa. The work is carried out for large countries or groups of small
163 countries, as inversions do not have the capability to constrain fluxes over small areas given their coarse
164 grid and sparse atmospheric data. Based on the benchmarking and relative merits evaluation of the
165 various data products presented above, the scientific questions addressed in this study are: 1) How
166 consistent are the mean values and trends of GHG emissions across BU estimates in Africa? 2) How
167 consistent are the different inversion model results? 3) How do inversions compare with BU estimates?
168 4) What is the net GHG balance of the African continent from different observation-based methods,
169 including CO₂ sinks and sources in the land-use sector? 5) What are the main sources of uncertainties?
170 The manuscript is organized into two main sections. First, a material and methods section describes the
171 regional breakdown and input data (section 1). We present our results for the whole Africa and for six
172 groups of aggregated countries (section 2) with a specific analysis of CO₂ emissions and sinks, divided
173 between FCO₂ (section 2.1), fluxes in the land use, land use change and forestry (LULUCF) sector
174 (section 2.2), and emissions of non-CO₂ greenhouse gasses (sections 2.3 and 2.4). Conclusions are
175 drawn about uncertainties of African GHG net emissions and removals assessment.

177 **1 Methods, datasets and datasets usage**

178
179 This study covers the period from 1990 to 2018, and emissions and sinks of CO₂, CH₄ and N₂O. We
180 used 1990 as a base year since reporting to the UNFCCC mostly started in that year and is often used
181 as a reference comparison year in national pledges of the PA. The last year of analysis is 2018,
182 reflecting the availability of inversion data and avoiding further uncertainty due to poorly understood

183 emissions changes before and after the COVID19 crisis. This period allows the analysis of decadal
184 features. It also has the advantage of being covered by several datasets, listed in Table 1. We considered
185 different BU approaches, including official countries communications to the UNFCCC and estimations
186 from the Food and Agriculture Organization (FAO), global inventories for anthropogenic emissions
187 (PRIMAP-hist which integrates combinations of various datasets including FAO, GCP, EDGAR
188 v4.3.2, Andrew 2018 cement data, BUR, Common Reporting Format (CRF), UNFCCC data, and BP),
189 and process-based models for land CO₂ fluxes with 14 Dynamic General Vegetation Models (DGVM)
190 from the TRENDY version 9 ensemble (Table 1). We used three atmospheric global inversions for CO₂
191 land fluxes; 22 inversions for CH₄ emissions; and three inversions for N₂O fluxes (Table 1). For
192 preliminary data quality control, we checked the consistency of prior fluxes by plotting them separately
193 (Fig. S1). Inversions only solve for total fluxes or at best for groups of sectors, whereas BU estimates
194 have a larger number of sectors. In Table 2, we present the correspondence between ‘sectors’ defined
195 by the TD and BU methods. For all datasets, we chose an atmospheric convention with negative values
196 representing removals from the atmosphere (i.e. land sink). No specific standard guidelines currently
197 exist for defining uncertainties of BU and TD data products. Given that some of our estimates are based
198 on a small number of models / estimates, we cannot calculate the full distribution e.g. with a 95%
199 confidence interval, but we rather reported ranges with min / max. Assuming that the unknown
200 distributions would be Gaussian, like in Schulze et al. (2018), we could infer a 2-sigma (\approx 95%)
201 confidence interval if we assume that min-max are equivalent to 3-sigma, but in view of the small
202 numbers of estimates e.g. for N₂O with only 3 inversions, we prefer to just give the min-max range.
203 Moreover, for national inventories, as all African countries are non-Annex I, they do not deliver
204 confidence intervals but Grassi et al. (2022) estimated for CO₂ LULUCF fluxes uncertainties of 50 %
205 for the average of non-Annex-1 countries. Here uncertainty estimates are understood as the spread
206 among minimum and maximum values from one methodology. A main source of uncertainty in the
207 comparison of country-reported data with other data products is the inclusion or not of natural fluxes
208 additionally to anthropogenic emissions sectors. For the comparability of the different data products
209 presented in this study, we discuss only the mean value over the period of overlapping data availability.
210 Referenced datasets are available at <https://doi.org/10.5281/zenodo.7347077> (Mostefaoui et al., 2022).

215 **Table 1. List of BU and TD methods used. (For more details, see also Saunois et al. (2020) for CH₄, Friedlingstein et**
 216 **al. (2020) for FCO₂; UNFCCC country-reported data; Gütschow et al. (2021) for PRIMAP-hist).**
 217

Dataset name	Method	CO ₂	CH ₄	N ₂ O	Spatial resolution	Time period covered
Inversions						
Global Carbon Budget ensemble (2020) ⁽¹⁾	TD	×			from 1° × 1° to 6° × 4°	2000-2019
Global Methane Budget ensemble ⁽²⁾ (2020)	TD		×		from 1° × 1° to 6° × 4°	2000-2017 ⁽³⁾
Global N₂O Budget ensemble ⁽⁴⁾ (2020)	TD			×	from 2.8° × 2.8° to 5.6° × 5.6°	1998-2017
DGVMs						
TRENDYv9 ⁽⁵⁾	BU				0.5° × 0.5° (land surface) or 1° × 1°	1990-2019
Other BU inventories						
PRIMAP-hist (excluding LULUCF)	BU	×	×	×	country	1990-2019
GCB (CDIAC) (excluding LULUCF)	BU	×			0.1° × 0.1°	1990-2019
UNFCCC	BU	×			country	1990-2015
FAO (LULUCF CO₂)	BU	×			country	1990-2019
GFEDv4 (wildfires only)	BU		×		0.25° × 0.25°	1997–2016

(1) See 3 inversions details in the supplementary Table S6.

(2) See 22 inversions details in the supplementary Table S7.

(3) Variations from 2003-2015, 2000-2015, 2010-2017: see detailed period coverage for each dataset in the supplementary Table S7.

(4) See 3 inversion details in the supplementary Table S8.

(5) See supplementary Table S5 for the 14 products.

218

219

220 **Table 2. Sectoral reconciliation between categories defined in TD and BU methods.**

Gas	Sector label choice for BU and TD	TD inversions	BU inventories
CO₂	Net land flux	Total Net Biome Productivity (NBP) after subtraction of prior prescribed Fossil CO ₂	Energy + Industrial Processes and Product Use + Agriculture + Waste + Biomass burning
CH₄	Total anthropogenic emissions	Fossil + Anthropogenic Biomass burning + Agriculture & Waste - Wildfires	Energy + Industrial Processes + Agriculture + Waste + Biomass burning
N₂O	Total	Total	All IPCC sectors

221 **1.1 Regional breakdown**

222 As some countries are small emitters and their area is too small to be resolved by inversions, and in some
 223 cases even by DGVMs, we grouped African countries into six regions shown in Fig. S2 and listed in Table
 224 S2. The grouping followed national borders and biomes similarity considering the Köppen-Geiger climate
 225 zones (Beck et al., 2018), magnitudes of fossil fuel emissions, and per capita emissions (Fig. S2, Fig. S3
 226 and Fig. S8). We also grouped a maximum of about ten countries per region.

227
 228 **1.2 Inventories datasets**

229 **PRIMAP-hist anthropogenic emissions assessment for CO₂, CH₄, and N₂O**

230 The PRIMAP-hist version 2.2 BU dataset is derived from Gütschow et al., (2021) and combines UNFCCC
 231 reports with a gap-filling method to produce a time series of annual anthropogenic emissions for different
 232 IPCC sectors. PRIMAP-hist does not cover the LULUCF sector for CO₂ due to the high uncertainties.
 233 PRIMAP-hist does not include emissions from shipping and international aviation, but includes cement as
 234 part of FCO₂ emissions. We use data from the HISTCR scenario (data accessed from <https://www.pik-potsdam.de/paris-reality-check/primap-hist/> in April 2022) from country-prioritized dataset, which mainly
 235 uses UNFCCC (BUR and NC) data, unless such data are missing, in that case PRIMAP-hist uses
 236 extrapolated data from EDGAR (2021), FAO (2021) and BP Statistical Review of World Energy (2021).
 237
 238

239 **Global Carbon Project (GCP) fossil CO₂ emissions**

240 We used country-level FCO₂ data published by the global CO₂ budget by the Global Carbon Project (GCP)
241 (Friedlingstein et al., 2020) separated per fuel type (gas, oil and coal) and including fossil fuel use in the
242 combined industry, ground transportation and power sectors, natural gas flaring, cement production, and
243 process-related emissions (e.g. fertilizers and chemicals). Data for African countries coming among others
244 from the Carbon Dioxide Information Analysis Center (CDIAC) compiled until 2018 (Gilfillan &
245 Marland, 2021), BP Statistical Review of World Energy (BP, 2020), and recent estimates of cement
246 production and clinker-to-cement ratios (Andrew, 2020).

247
248 **UNFCCC inventories for CO₂ in the LULUCF sector**

249 We used UNFCCC submissions for LULUCF CO₂ fluxes from NC and BUR reports downloaded from
250 the UNFCCC website (<https://unfccc.int/>) in March 2021, and further processed into .csv tables by Deng
251 et al., (2021). Those estimates are based on different accounting methods following the IPCC Guidelines
252 (IPCC, 2006; IPCC, 2019). Country-reported data quality control, quality assurance and verification
253 process follow 2006 IPCC guidelines detailed in Chapter 6 QA/QC procedures of this document. African
254 countries, being Non-Annex I countries, do not report emissions every year. Figure 1 shows the number
255 of BUR and NC provided each year per African region. The years 1990, 1994, 1995, 2000 and 2005 are
256 featured with several updates, while most of the other years have few updates. About every two years, all
257 regions have at least one update. Note that flexibility for BUR is given to Least Developed Countries
258 (LDCs), that include 33 out of 56 African countries, and to Small Islands Developing States (SIDS), that
259 include six African countries (Table S4).

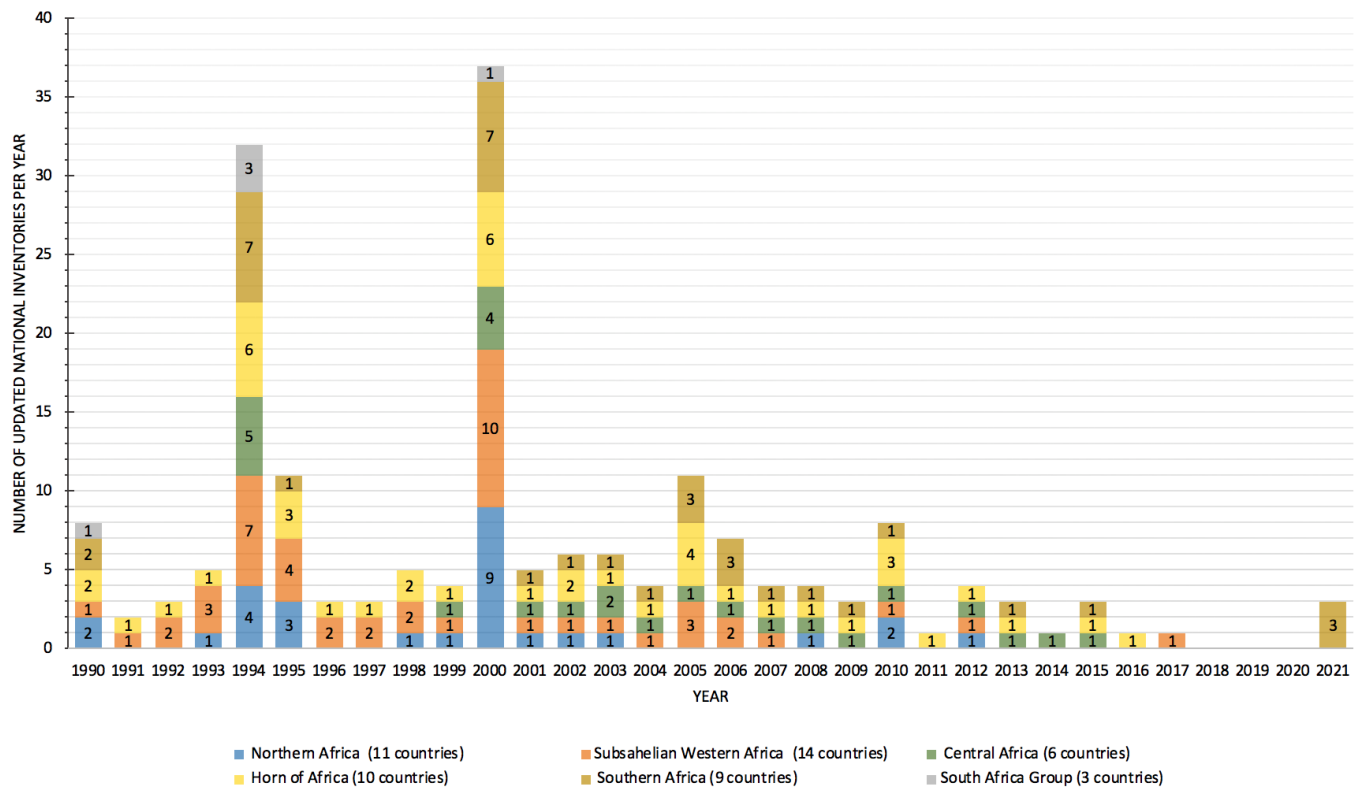


Figure 1. Number of UNFCCC reports for LULUCF CO₂ fluxes in National Communications and Biennial Update Reports, per group of countries defined in Table S2.

Non-Annex I African countries can use older versions of the IPCC guidelines (IPCC, 2006; IPCC, 2019a). This induces uncertainties from changes in accounting methods between versions, with recent guidelines having more detailed sectors and sources. There is no data for Libya, Equatorial Guinea, Malawi and Sierra Leone during the whole period. UNFCCC data are missing in some years for Rwanda, Sao Tome & Principe, Senegal, South Sudan, Angola. There is no data during 1990-1998 for Liberia.

We noticed that NC and BUR lack details regarding the methods used, the sources for activity data and emissions factors, and most of them are in French language. BUR in .pdf format include a non-standardized table for emissions. The reader is sometimes referred to the “national coordinator for climate change service” with no link to any database or contact person.

Because the PA targets human-induced emissions, countries use the proxy of “Managed lands” for the LULUCF sector, as defined by the IPCC guidelines (<https://www.ipcc-nggip.iges.or.jp/public/2006gl/vol4.html>; last accessed in August 2022). Managed lands are areas where LULUCF CO₂ fluxes are assigned to some anthropogenic activities. Several African NC and BUR do not contain information on their managed lands areas. We thus looked at REDD+ national reports (<https://redd.unfccc.int/submissions.html?topic=6>; last accessed in August 2022) to get this information

279 (Fig. S3 and Table S9). LULUCF CO₂ fluxes on managed lands result from either direct anthropogenic
280 effect such as land use change and forestry, or indirect effects (such as change in CO₂ and climate) on land
281 remaining in the same land use, e.g. forest remaining forest (Grassi et al., 2022). The vast majority of African
282 countries use a Tier 1 IPCC accounting method which does not distinguish between these different effects.
283 Tier 1 methods use a classification with only three out of six possible types of land: “forest land”, “cropland”
284 and “grassland”, and do not give spatially explicit land use data. Tier 2 methods include fluxes from six
285 land use types: forest, cropland and grassland, wetlands, urban and other land-use, for the case of land
286 remaining under the same land use type, and for the case of conversions between land use types. In Africa,
287 only South Africa and Zambia used Tier 2 methods for some LULUCF CO₂ subsectors.

288 **Processing of the UNFCCC LULUCF CO₂ data and outliers correction**

289 We processed the UNFCCC LULUCF CO₂ data for outlier corrections (Table S5). For Guinea-Bissau, and
290 Tanzania, we identified inconsistent values from successive communications with substantially differing
291 numbers. For Guinea, Madagascar, Zimbabwe, Congo, Mali, the Central African Republic (CAF), Angola
292 and Mauritius we identified changes of more than one order of magnitude between two consecutive reports
293 and likely implausibly large carbon sinks considering their national forest area. The computations of per
294 area emissions and removals showed discrepancies, which points out the need for further examination and
295 inspection of more recent reports in NDC and REDD+ reports (Table S5). Our corrections explained in the
296 supplementary section are consistent with those proposed by Grassi et al. (2022) who diagnosed
297 ‘biophysically impossible’ sequestration rates with a threshold value larger than 10 tCO₂/ha yr⁻¹ over an
298 area greater than 1 Mha. For Namibia, Nigeria and the Democratic Republic of the Congo (DRC), it was
299 challenging to select a best estimate between recent and past reports. For those countries, corrections using
300 more recent data than BUR/NC have high uncertainties, as noted by Grassi et al. (2022). This includes the
301 absence of any sink for DRC for instance, contrary to sinks consistently reported over time and large forested
302 area in this country’s previous reports to the UNFCCC. We therefore systematically looked at corrected
303 values for both case scenarios (with and without Namibia, Nigeria and DRC data corrections). In total, we
304 corrected 13 outliers as shown in Table S5, consistently with Grassi et al. (2022).

305 **Food and Agriculture Organization of the United Nations (FAO) LULUCF CO₂ fluxes**

306 We used data from LULUCF CO₂ fluxes over 1990-2019 from the FAO Global Forests Resource
307 Assessments (FAOSTAT, available at: <https://www.fao.org/faostat/en/#data/GT>; last access: May 2022,
308 2022). According to the 2005 FAO categories and definitions, forest is land covering at least 0.5 hectares
309 and having vegetation taller than 5 meters with a canopy cover higher than 10%. Other wooded lands refer
310 and having vegetation taller than 5 meters with a canopy cover higher than 10%. Other wooded lands refer
311

312 to land that are not classified as “forest” but that are wider than 0.5 ha, have a canopy cover of 5%-10% or
313 combine trees, shrubs and bushes with cover higher than 10%. The FAO data for forests comprise carbon
314 stock changes from both aboveground and belowground living biomass pools. They are independent from
315 country-reported UNFCCC emissions and removals. The FAO estimates are based on activity data, areas of
316 forest land and CO₂ emissions and removals factors. The FAO data reports: 1) net emissions and removals
317 from “forest land remaining forest land” and from “land converted to forest” grouped together, and 2)
318 emissions from "net forest conversion", i.e. deforestation. In contrast, the UNFCCC accounting uses a 20-
319 years window for CO₂ fluxes from land use change, while land-use change fluxes from land-converted-to-
320 forest are reported separately from those of ‘forest remaining forest’.

321 **1.3 Dynamic Global Vegetation Models (DGVM) datasets**

322 We used Net Biome Productivity (NBP) from 14 Dynamic Global Vegetation Models (DGVM) from the
323 TRENDY v9 ensemble covering the period 1990-2019. The different models described in Friedlingstein et
324 al. (2019) are: CABLE, CLASS, CLM5, DLEM, ISAM, JSBACH, JULES, LPJ, LPX, OCN, ORCHIDEE-
325 CNP, ORCHIDEE-SDGVM, and SURFEX (Table S6). DGVM are forced by historical reconstructions of
326 land cover change, atmospheric CO₂ concentration and climate since 1901. Detailed cropland management
327 practices are generally ignored, except for the harvest of crop biomass. Forest harvest is prescribed from
328 historical statistics in 11 models (Table A1, of Friedlingstein et al., (2020)). The models simulate carbon
329 stock changes in biomass, litter and soil pools. From the difference between simulations with and without
330 historical land cover change, a flux called ‘land use emissions’ can be obtained from DGVM. This flux
331 includes the indirect effects of climate and CO₂ on lands affected by land use change, and a foregone sink
332 called “loss or gain of atmospheric sink capacity”, which is absent from the methods used by UNFCCC and
333 FAO. Pongratz et al. (2014) delivered the following definition of loss of sink capacity as “the CO₂ fluxes in
334 response to environmental changes on managed land as compared to potential natural vegetation.
335 Historically, the potential natural vegetation would have provided a foregone sink as compared to human
336 land use.” Thus, land use change fluxes from DGVM were not compared with other estimates. Note that
337 DGVM do not explicitly separate managed and unmanaged land. Thus, we used all forest lands to calculate
338 their mean CO₂ fluxes.
339
340

341 **1.4 Atmospheric inversions datasets**

342 **CO₂ inversions**

343

344 We used the net land CO₂ fluxes excluding fossil fuel emissions (hereafter, net ecosystem exchange) from
345 three global inversions of the Global Carbon Project that cover a long period (see Table A4 of Friedlingstein
346 et al., 2020), including : CarbonTrackerEurope (CTRACKER-EU-v2019; van der Laan-Luijkx et al., 2017),
347 the Copernicus Atmosphere Monitoring Service (CAMSV18-2-2019; Chevallier et al., 2005), and one
348 variant of Jena CarboScope (JENA, sEXTocNEET_v2020; Rödenbeck et al., 2005). The GCP inversion
349 protocol recommends to use as a fixed prior the same gridded dataset of FCO₂ emissions (GCP-GridFED).
350 However, some modelers used different interpolations of this dataset, and one group used a different gridded
351 dataset (Ciais et al., 2021). We applied a correction to the estimated total CO₂ flux by subtracting a common
352 FCO₂ flux from each inversion (Figure S1 and Methodological Supplementary 1). The resulting land
353 atmosphere CO₂ fluxes, or net ecosystem exchange, cannot be directly compared with inventories aiming
354 to assess C stock changes, given the existence of land-atmosphere CO₂ fluxes caused by lateral processes.
355 This issue was discussed by Ciais et al. (2021) and a practical correction of inversions was proposed by
356 Deng et al. (2022) based on new datasets for CO₂ fluxes induced by lateral processes involving river
357 transport, crop and wood product trade. We applied here the same correction to all CO₂ inversions.

358 **CH₄ inversions**

359 We used the CH₄ emissions from global inversions over 2000-2017 from the Global Methane Budget
360 (Saunois et al., 2020) (Table 1). This ensemble includes 11 models using GOSAT satellite CH₄ total-column
361 observations covering 2010-2017, and 11 models assimilating surface stations data (SURF) since 2000
362 (Table S5). Surface inversions are constrained by very few stations for Africa, while the GOSAT satellite
363 data has a better coverage. One could thus expect GOSAT inversions to give more robust results. Inversions
364 deliver an estimate of surface net CH₄ emissions, although some of them solve for fluxes in groups of
365 sectors, called ‘super-sectors’. We have not used in situ for dataset validation per se, only the GOSAT data
366 were evaluated against Total Carbon Column Observing Network (TCCON) independent ground based total
367 column-averaged abundance of CH₄ (XCH₄). In the inversion dataset, net CH₄ surface emissions were
368 interpolated into a 0.8° × 0.8° resolution, regridded from coarser resolution fluxes and separated into ‘super-
369 sectors’ either using prior emission maps or posterior estimates for those inversions solving fluxes per
370 supersector, following Saunois et al. (2020). More specifically, these five super-sectors are: 1) Fossil Fuel,
371 2) Agriculture and Waste, 3) Wetlands, 4) Biomass and Biofuel Burning (BBUR), and 5) Other natural
372 emissions. We separated CH₄ anthropogenic emissions from inversions using Method 1 and Method 2
373 proposed by Deng et al. (2021). Method 1 relies on the separation calculated by each inversion except for
374 the BBUR supersector from which wildfire emissions were subtracted based on the Global Fires Emission
375 Dataset (GFED) version 4 (van der Werf et al., 2017). Method 2 removes from total emissions the median

376 of natural emissions from inversions (Deng et al. 2022). The two methods gave similar results and only
377 Method 1 was used in the results section.

379 **N₂O inversions**

380 We used three N₂O atmospheric inversions from the global N₂O budget synthesis (Tian, 2020) and from
381 Deng et al. (2022) (Tables S1 and S7) : PyVAR CAMS (Thomson et al., 2014), MATCM_JMASTEC
382 (Rodgers, 2000), (Patra et al., 2018), and TOMCAT (Wilson et al., 2014; Monks et al., 2017). We used the
383 total N₂O flux from inversions including natural emissions, given that natural emissions estimates are highly
384 uncertain for Africa. Inversion results are therefore not directly comparable with the PRIMAP-hist inventory
385 which only contains anthropogenic emissions.

387 **1.5 Metrics to compare gasses and ancillary data and data usage**

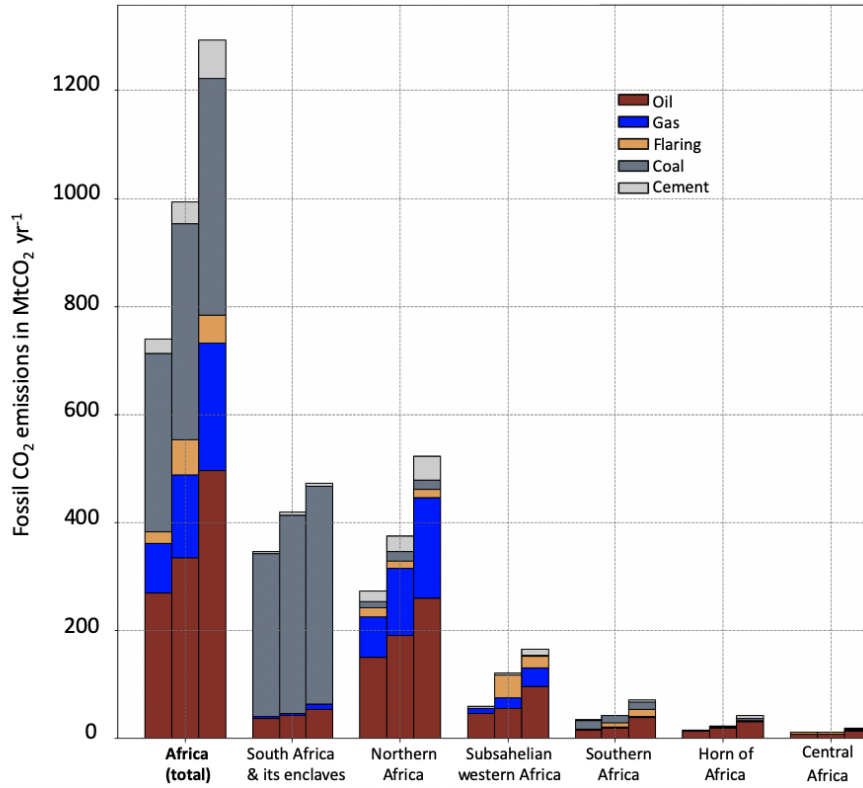
388
389 We express emissions of non-CO₂ gasses in megatons of carbon dioxide equivalent (MtCO₂e) using the
390 Global Warming Potential over a 100-year time horizon (GWP100) values from the fourth IPCC
391 Assessment Reports (IPCC AR4, WGI Chapter 2, 2007), consistent with PRIMAP-hist and historical
392 country-reported data. We used AR4 GWP100 because many African countries have been following the
393 2006 IPCC guidelines referring to AR4 GWP100 2019 refinement to IPCC guidelines, which do not
394 recommend any specific metrics, therefore we are following IPCC guidelines used by countries. The
395 multiplicative coefficients to use to change AR4 to AR6 GWP100 values are: 1.19 for fossil CH₄, 1.09 for
396 non-fossil CH₄, and 0.92 for N₂O. We used population data from the United Nations population (World
397 Population Prospects 2019, 2022), for computing per capita FCO₂ emissions and their disparities, based on
398 Gini indices (Dortman et al., 1979) for measuring statistical dispersions among a given population
399 (methodological supplementary M2). We also used African GDP data (World Bank, 2017).

401 **2 Results and discussion**

402 **2.1 Fossil CO₂ emissions**

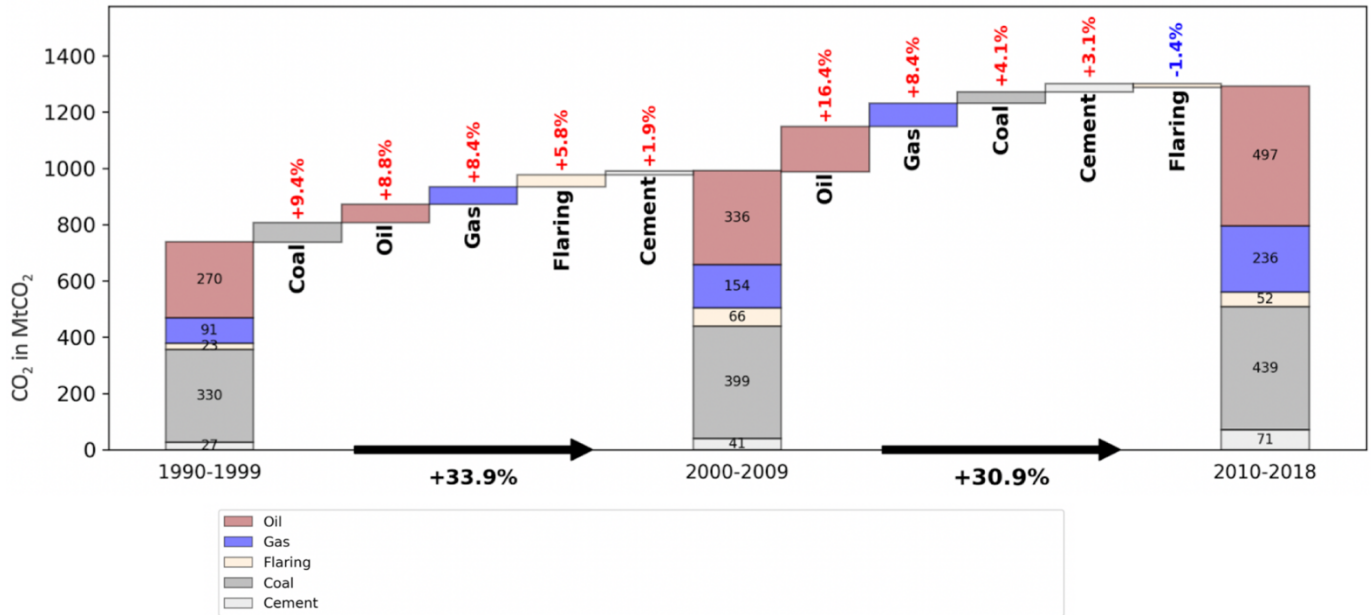
403 **2.1.1 Continental, regional and country changes**

409 (a)



410 (b)
411

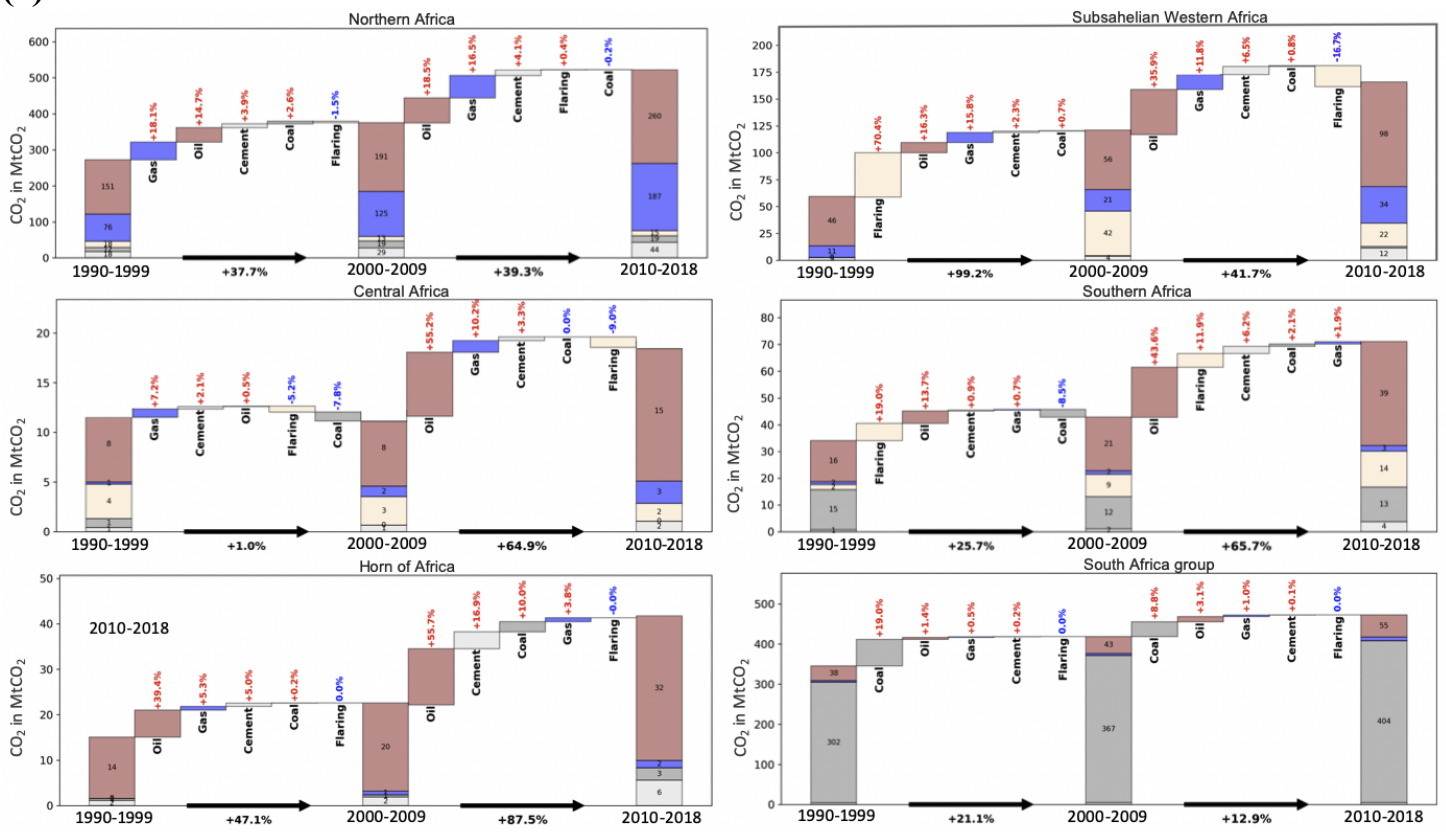
Total Africa CO₂ emissions by sector - GCP



412
413
414
415

416

(c)



417

418

419

420

421

422

423

424

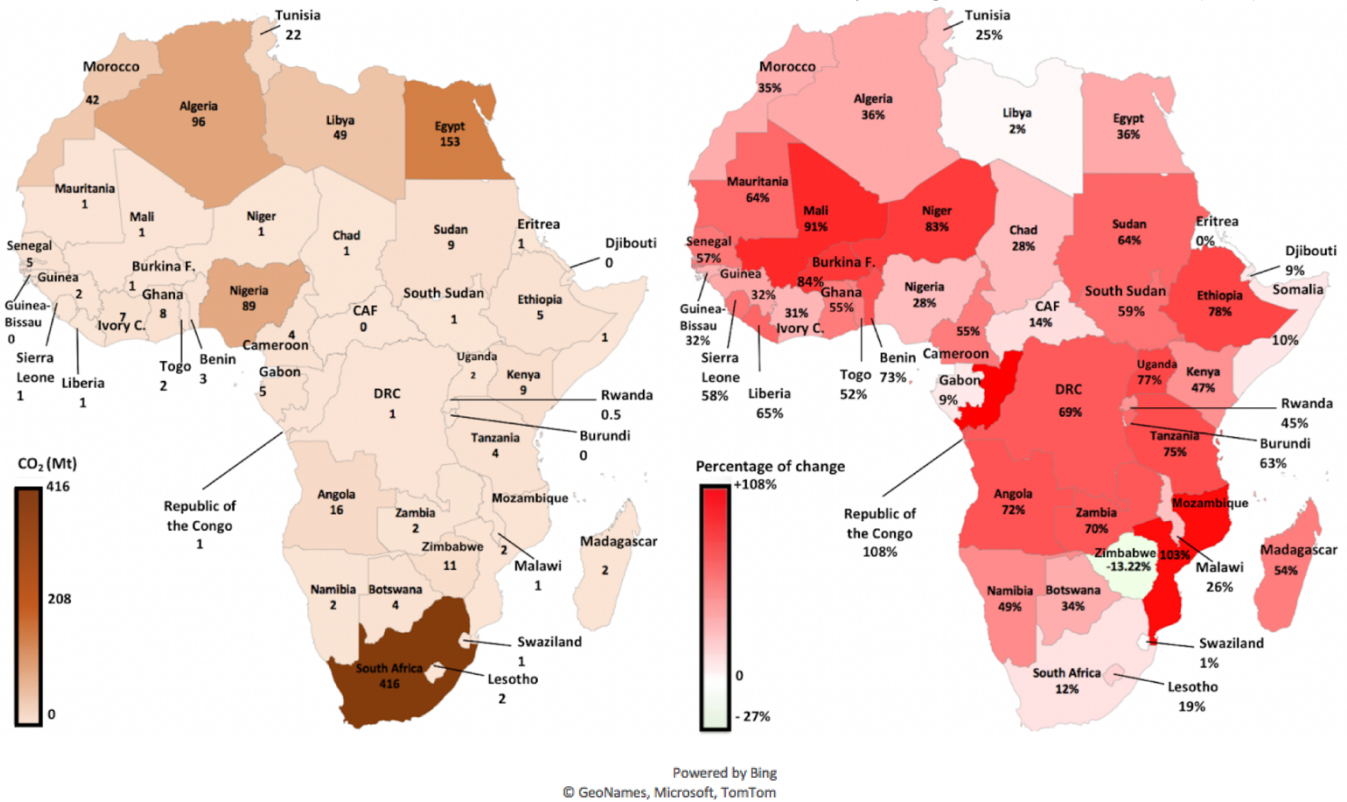
425

426

427 Figure 2. (a) African fossil fuel CO₂ emissions per fuel type and for cement per region over 1990-1999, 2000-2009
 428 and 2010-2018. (b) Contribution of each fuel type to the change of African emissions. (c) Same for different regions
 429 regrouping several countries. Data from GCP (2019).

430 (a) FCO₂ total anthropogenic emissions mean
 431 1999-2008 in Mt yr⁻¹ (GCP).
 432

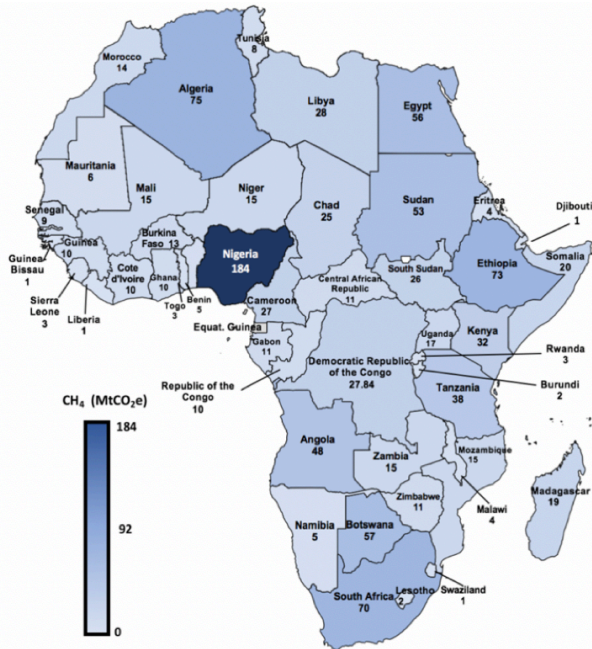
(b) Differences expressions in percentage between FCO₂ total
 anthropogenic mean emissions 2009-2018 and mean 1999-2008
 divided by average value for both decades (GCP).



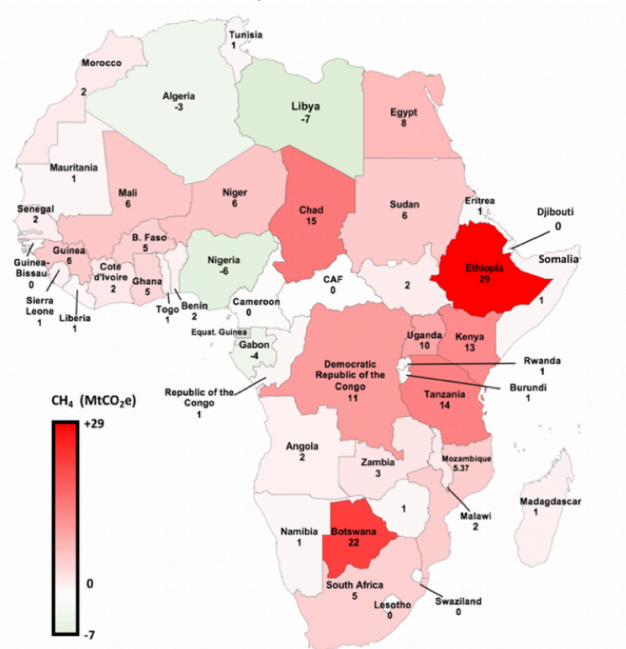
433
 434
 435
 436
 437
 438
 439
 440
 441
 442
 443
 444
 445
 446
 447
 448
 449

450
451
452

(c) CH₄ total anthropogenic emissions mean 1999-2008 in MtCO₂e yr⁻¹ (PRIMAP-hist).



(d) Differences between CH₄ total anthropogenic mean emissions 2009-2018 and mean 1999-2008 in MtCO₂e yr⁻¹ (PRIMAP-hist).



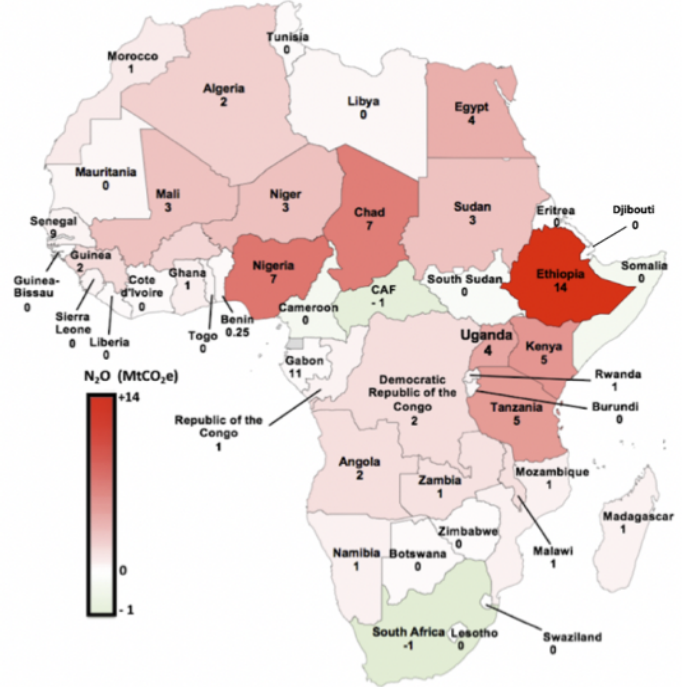
Powered by Bing
© GeoNames, Microsoft, TomTom

453
454
455
456
457
458
459

(e) N₂O total anthropogenic emissions mean 1999-2008 in MtCO₂e yr⁻¹ (PRIMAP-hist).



(f) Differences between N₂O total anthropogenic mean emissions 2009-2018 and mean 1999-2008 in MtCO₂e yr⁻¹ (PRIMAP-hist).



Powered by Bing
© GeoNames, Microsoft, TomTom

460
461

462 **Figure 3 (a). Maps of average fossil fuel CO₂ emissions for African countries during 1999-2008 in MtCO_{2e} yr⁻¹ and**
463 **(b) change from 1999-2008 to 2009-2018 using data from GCP in MtCO_{2e} yr⁻¹ (Friedlingstein et al., 2019); (c-d)**
464 **same but with anthropogenic CH₄ emissions from PRIMAP-hist in MtCO_{2e} yr⁻¹; (e-f) same for anthropogenic N₂O**
465 **emissions from PRIMAP-hist in MtCO_{2e} yr⁻¹.**

466

467 **PRIMAP-hist and GCP**

468 First, we compared GCP and PRIMAP-hist fossil CO₂ emissions. We found that most of the relative differences
469 between these two datasets at country level considerably decreased with time, except for Mali. Those
470 differences are less than 5% for most of the main African emitters during the last decade, except for South
471 Africa where the difference is a bit larger than 10% (see maps in Fig. S8). The largest relative difference
472 between the two datasets comes from Mali in the decade 2009-2018, with FCO₂ emissions of 3 MtCO₂ yr⁻¹ in
473 GCP, compared to 1 MtCO₂ yr⁻¹ in PRIMAP-hist. Given the relatively small differences, we chose to use only
474 GCP for trends between decades, but when computing net budgets for the three main GHG, we show
475 differences between the use of those two estimates.

476 The changes of African FCO₂ emissions per fuel type and for cement using the GCP data are shown in Fig. 2
477 (a). In Fig.2 (b), we show absolute values and relative contributions to the total change in each decade. During
478 2010-2018, total African FCO₂ emissions from oil (497 MtCO₂ yr⁻¹) and coal (439 MtCO₂ yr⁻¹) were roughly
479 similar. While global FCO₂ emissions increased by +13 % over this period (Friedlingstein et al., 2019), African
480 FCO₂ almost doubled in 2018 compared to 1990 levels, a relative increase comparable with that of China over
481 the same period. From 1990-1999 to 2000-2009, the mean emissions increased by 33.9% from 741 MtCO₂ yr⁻¹
482 to 996 MtCO₂ yr⁻¹. All FCO₂ sectors contributed to this decadal increase. The contribution from coal (+9.4
483 %) was slightly larger but comparable to that from oil (+9 %) and gas (+8 %). From 2000-2009 to 2010-2018,
484 emissions further increased by 31% from 996 MtCO₂ yr⁻¹ to 1295 MtCO₂ yr⁻¹. The oil and the gas fuels
485 contributed the most to this increase with +16 % for oil, and +8 % for gas. Coal emissions increased by only
486 +4.1 % and coal went from being the first source of African FCO₂ emissions over 2000-2009 to the second one
487 over 2010-2018.

488 As for regional contributions to emissions changes between 1990-1999 and 2000-2009 shown in Fig. 2 (b) the
489 main contribution to the total increase came from the region of South Africa where emissions increased from
490 302 MtCO₂ yr⁻¹ to 367 MtCO₂ yr⁻¹ (+21.1 %, coal being the largest contributor). The second largest contribution
491 to the increase is from North Africa where oil was the largest contributor (emissions increased from 151 MtCO₂
492 yr⁻¹ to 191 MtCO₂ yr⁻¹; +15 %), and gas (+18%). The least increasing region was Central Africa. North Africa

493 experienced the largest increase from 1990-1999 to 2000-2009, and from 2000-2009 to 2010-2018 with
494 successive increases of +38 % and +39 %, largely dominated by oil and gas (Fig. 4 (b)). As a result, during the
495 period 2010-2018, Northern African countries were the dominant emitters with 545 MtCO₂ yr⁻¹. The group of
496 South Africa (including Lesotho and Botswana) was the second biggest emitter region over 2010-2018, mainly
497 due to coal emissions from the Republic of South Africa. The two least contributing African regions were the
498 Horn of Africa and Central Africa.

499 At the country level, Figure 3a-b shows mean FCO₂ emissions and relative changes over the last two decades.
500 The main emitters do not have the biggest relative changes. The four main emitters over 2000-2009 were South
501 Africa (416 MtCO₂ yr⁻¹), Egypt (153 MtCO₂ yr⁻¹), Algeria (96 MtCO₂ yr⁻¹) and Nigeria (89 MtCO₂ yr⁻¹). Those
502 four countries altogether represented 67% of the continental total emissions over 2000-2009 (987 MtCO₂ yr⁻¹).
503 The largest relative increases from 2000-2009 to 2010-2018 are from Congo (+108 %), Mozambique (+103 %)
504 and Mali (91%), compared to relative increases in the main emitters, the Republic of South Africa (+21 %),
505 Egypt (+36%) and Algeria (+36%).

506

507 **2.1.2 Variations of per capita and per GDP fossil fuel CO₂ emissions**

508

509 **Per capita emissions**

510 Using ancillary data on population (Fig. S3 and Fig. S4) we computed the mean African per capita emissions
511 of 1 tCO₂/cap yr⁻¹ for 2009-2018, which is 5 times larger than during 1990-1998 (0.2 tCO₂/cap yr⁻¹), and yet 5
512 times smaller than the global average (5 tCO₂/cap yr⁻¹). From 1999-2008 to 2009-2018, African per capita
513 emissions increased by 30 %. African per capita FCO₂ emissions during 2009-2018 were 17 times less than in
514 the USA (17 tCO₂/cap yr⁻¹), 7 times less than in China (7 tCO₂/cap yr⁻¹), 7 times less than in EU27+UK (7
515 tCO₂/cap yr⁻¹), and 2 times less than India (2 tCO₂/cap yr⁻¹). At the country level, the biggest per capita emissions
516 over 2009-2018 were from the Republic of South Africa with 9 tCO₂/cap yr⁻¹, which ranks 14th worldwide,
517 above China and just below Poland. The second biggest per capita emissions were from Libya (8 tCO₂/cap yr⁻¹).
518 The smallest ones were from the DRC (0.1 tCO₂/cap yr⁻¹). For the first period 1990-1998, per capita
519 emissions of African region ranked in this order: South Africa group (4 tCO₂/cap yr⁻¹) > Northern Africa (2
520 tCO₂/cap yr⁻¹) > Central African countries (1 tCO₂/cap yr⁻¹) > Southern countries (0.8 tCO₂/cap yr⁻¹) > Horn of
521 Africa (0.5 tCO₂/cap yr⁻¹) > Sub-Saharan Western Africa (0.3 tCO₂/cap yr⁻¹). For the second period 2009-2018,
522 they ranked in this order: South Africa group (4 tCO₂/cap yr⁻¹) > Northern Africa (2 tCO₂/cap yr⁻¹) > Southern
523 countries (1 tCO₂/cap yr⁻¹) and Horn of Africa (1 tCO₂/cap yr⁻¹) > Central Africa countries (1 tCO₂/cap yr⁻¹) >
524 Sub-Saharan Western Africa (0.4 tCO₂/cap yr⁻¹). At country scale during the first period of 1990-1998, the

525 four African largest per capita emissions ranked in this order: Libya (9 tCO₂/cap yr⁻¹ > the Republic of South
526 Africa (9 tCO₂/cap yr⁻¹) > Gabon (5 tCO₂/cap yr⁻¹) > Algeria (3 tCO₂/cap yr⁻¹). The four African countries with
527 the smallest per capita emissions ranked as following: Burundi (0.04 tCO₂/cap yr⁻¹) < Uganda, Ethiopia and
528 Mali (0.1 tCO₂/cap yr⁻¹).

529 We also computed the GINI index for African per capita FCO₂ emissions for each of the last three decades,
530 using data from (Friedlingstein et al., 2020) (see Methodological Supplementary M2). These GINI values were
531 0.7 for 1990-1998, 0.7 for 1999-2008, and 0.7 for 2009-2018, thus very stable over the last 30 years and close
532 to 1, indicating high inequities among countries.

533 **Emissions per GDP**

534 **Per exchange rate vs. per Purchasing Power Parities (PPP) GDP**

535 According to the International Monetary Fund (IMF), the Gross Domestic Product (GDP) delivers an estimate
536 “of the monetary value of goods and services produced in a country over a chosen period.” GDP data from the
537 World Bank (2015) is available for 30 African countries only (Fig. S5). The four countries with the biggest per
538 \$US exchange rate GDP (Fig. S6) are: Nigeria (\$490 B) > South Africa (\$350B) > Egypt (\$330B) and Algeria
539 (\$330B) > Angola (\$120B). The four countries with the smallest GDP in 2015 are: Gambia (\$1.4B) and
540 Seychelles (\$1.4B) > Guinea-Bissau (\$1B) > Comoros (\$970 M). Emissions per \$US GDP are shown in Fig.
541 S6 The Purchasing Power Parities (PPP) calculated by the International Comparison Program (ICP) of the
542 World Bank is a refined measure of what a given national currency can acquire in terms of goods or services
543 in another country, removing the impact of currency exchange rates. Emissions per PPP\$ GDP are shown in
544 Fig. S7.

545 The mean of African emissions per unit PPP\$ GDP in 2016 was 0.6 kgCO₂/PPP\$ yr⁻¹, which is more than twice
546 the global value, 3 times the mean value of the USA (0.2 kgCO₂/PPP\$ yr⁻¹), and Europe (0.2 kgCO₂/PPP\$ yr⁻¹).
547 This points to a more carbon intensive economic growth in Africa than in developed countries, which may
548 be an important barrier for future mitigation strategies as the GDP of Africa has grown by 112% in the last 30
549 years, and is projected to increase in the future by 3% per year (World Bank, 2022). At regional level, the
550 largest values were: South Africa (0.4 kgCO₂/PPP\$ yr⁻¹) > North Africa, Southern Countries and Sahelian
551 Western Africa (0.2 kgCO₂/PPP\$ yr⁻¹) > Central Africa and the Horn of Africa (0.1 kgCO₂/PPP\$ of GDP). At
552 country scale, the largest emitters per unit of GDP were Libya (0.7 kgCO₂/PPP\$ yr⁻¹) and South Africa (0.7
553 kgCO₂/PPP\$ yr⁻¹) > Lesotho (0.4 kgCO₂/PPP\$ yr⁻¹) > Algeria (0.3 kgCO₂/PPP\$ yr⁻¹) (Fig. S7.) The smallest
554 emitters were: DRC (0.03 kgCO₂/PPP\$ yr⁻¹) < Chad (0.04 kgCO₂/PPP\$ yr⁻¹) < Burundi (0.06 kgCO₂/PPP\$ yr⁻¹)
555 < Uganda (0.07 kgCO₂/PPP\$ yr⁻¹).

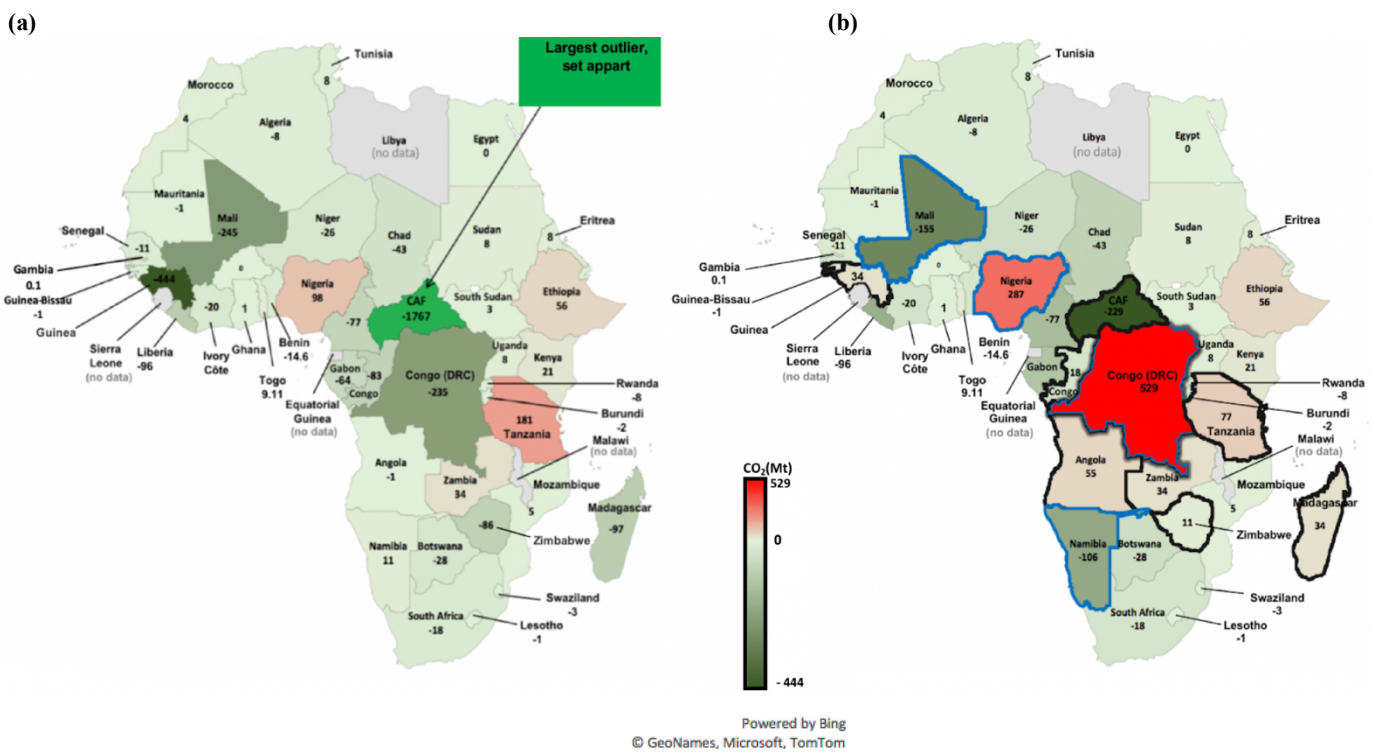
556 We also used GDP per unit exchange rate from the International Energy Agency (IEA, 2019). The mean African
 557 emissions per unit of $\text{GDP}_{\text{exch.rate}}$ was $0.5 \text{ kgCO}_2 / \$ \text{ yr}^{-1}$, larger than elsewhere, except in Asia ($0.6 \text{ kgCO}_2 /$
 558 $\text{GDP}_{\text{exch.rate}} \text{ yr}^{-1}$). As shown in Fig. S6, over 2013-2017 the six biggest emitters were South Africa ($0.7 \text{ kgCO}_2 /$
 559 $\text{GDP}_{\text{exch.rate}} \text{ yr}^{-1}$) > Libya ($0.5 \text{ kgCO}_2 / \text{GDP}_{\text{exch.rate}} \text{ yr}^{-1}$) > South Sudan ($0.4 \text{ kgCO}_2 / \text{GDP}_{\text{exch.rate}} \text{ yr}^{-1}$) > Zimbabwe,
 560 Benin and Algeria ($0.3 \text{ kgCO}_2 / \text{GDP}_{\text{exch.rate}} \text{ yr}^{-1}$). The correlation coefficient between $\text{GDP}_{\text{exch.rate}}$ and FCO_2
 561 emissions per $\text{GDP}_{\text{exch.rate}}$ was 0.3, suggesting that the countries with a high GDP do not always emit more CO_2
 562 per unit GDP. For instance, South Africa ranked first with $0.7 \text{ kgCO}_2 / \text{GDP}_{\text{exch.rate}} \text{ yr}^{-1}$ and second for GDP (350
 563 \$Billion); Nigeria ranked first for GDP (490 \$Billion), but 21st for emissions per GDP ($0.1 \text{ kgCO}_2 / \text{GDP}_{\text{exch.rate}}$
 564 yr^{-1}). This may be related to the fact that countries with a high GDP are also more likely to create growth
 565 through sustainable activities.

566

567 **2.2 LULUCF CO_2 fluxes**

568 **Outlier corrections**

569



570
 571
 572
 573
 574
 575
 576
 577
 578
 579
 580
 581

(c)

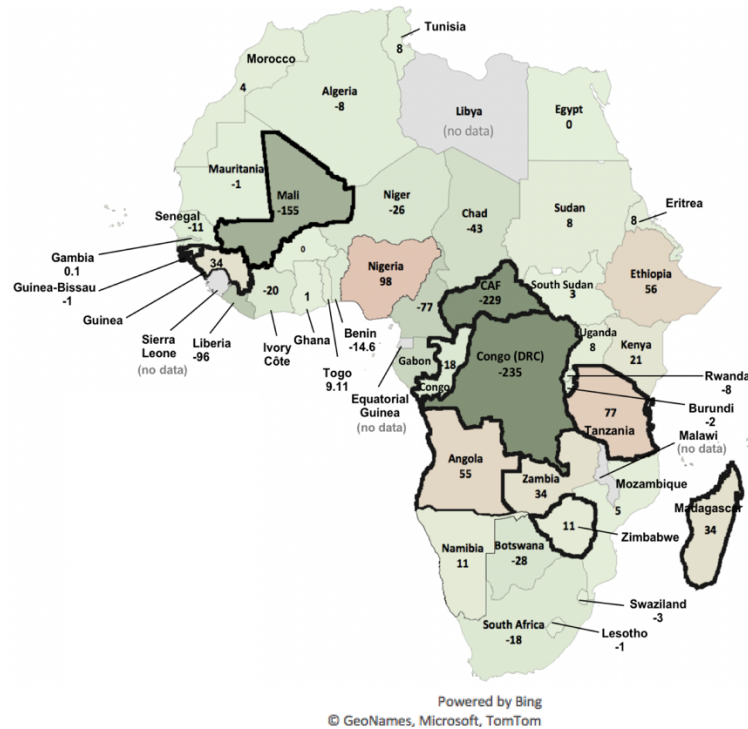


Figure 4. Map of national LULUCF CO₂ fluxes for 2001-2018 in MtCO₂ yr⁻¹. (a) Before outliers' removals. (b) After outliers' removal according to Grassi et al. (2022). (c) After outlier removals (DRC, Namibia and Nigeria) from this study. Positive values represent a net C loss by ecosystems.

In this section, we analyze CO₂ fluxes from the LULUCF sector, based on UNFCCC data (section 1.1) which include forest lands, grasslands, croplands, and all possible conversions between them (IPCC, 2003; 2006). As shown in section 1.2 and Table S4, we found that some countries' reports are outliers with biophysically implausible CO₂ sinks and/or sudden unexplained very large changes between successive reports. Due to scarce data over 1990-1998 we focus on the period 2001-2018. In the following paragraph, we discuss four approaches to include UNFCCC data:

a) Uncorrected data, b) corrections following Grassi et al. (2022) for all countries, c) corrections following Grassi et al. (2022) except DRC, Namibia and Nigeria, d) Corrections following Grassi et al. (2022) except for DRC.

Figure 4 (a) shows UNFCCC data without correcting for outliers, based on BUR and NC data accessed in May 2022. The majority of countries are sinks, or small sources, except Tanzania and Nigeria being large sources. Very large (implausible) sinks are seen in Guinea and CAF. The continent is a CO₂ sink of -3309 MtCO₂ yr⁻¹ during the period 2001-2018.

603 Figure 4 (b) shows the corrected fluxes according to Grassi et al. (2022) who excluded implausible large
604 sink rates and used NDC and REDD+ reports instead of NC data for DRC, Congo, CAF, Guinea,
605 Madagascar and the most recent BUR, NC and inventory data for Namibia, Angola, Zimbabwe and
606 Nigeria (see their Table 7). Africa as a whole is a CO₂ source of 265 MtCO₂ yr⁻¹. At regional scale, the
607 mean CO₂ sources distributes as follows on four regions: Sub-Saharan West Africa (235 MtCO₂ yr⁻¹) >
608 Horn of Africa (153 MtCO₂ yr⁻¹) > Central Africa (144 MtCO₂ yr⁻¹) > Southern Africa (14 MtCO₂ yr⁻¹).
609 The two sink regions are North Africa (-259 MtCO₂ yr⁻¹) and South Africa (-23 MtCO₂ yr⁻¹). At country
610 scale, after the corrections of Grassi et al. (2022), the four countries with the larger sinks are: CAF (-229
611 MtCO₂ yr⁻¹) > Mali (-155 MtCO₂ yr⁻¹) > Namibia (-106 MtCO₂ yr⁻¹) > Cameroon (-77 MtCO₂ yr⁻¹). The
612 four countries with largest sources are DRC (529 MtCO₂ yr⁻¹) > Nigeria (287 MtCO₂ yr⁻¹) > Tanzania
613 (77 MtCO₂ yr⁻¹) > Ethiopia (56 MtCO₂ yr⁻¹). A main issue with the correction from Grassi is that it reports
614 no sink in DRC which has an important forest coverage representing 68% of the country area (FAO,
615 2015) and for which a sink was consistently reported in previous NCs.

616 Figure 4 (c) shows LULUCF CO₂ in African countries that are consistent with Grassi et al. (2022) except
617 for three countries: Namibia (we used 2000 NC3 instead of NIR2019), Nigeria (we used 2014 NC2
618 instead of 2017 BUR2) and DRC (we used 2015 NC3 instead of 2021 NDC). In that approach Africa
619 becomes a net CO₂ sink of -589 Mt yr⁻¹ over 2001-2018. At regional scale, the region of Central Africa
620 (-620 MtCO₂) remains the main sink. But the values and ranking of the top sources rank as: Horn of
621 Africa (153 MtCO₂) > Southern Africa (141 MtCO₂) > Sub-Saharan West Africa (19MtCO₂). At country
622 scale with this correction choice, the top sinks are: DRC (-235 MtCO₂) > CAF (-229 MtCO₂) > Mali (-
623 155 MtCO₂); and the three top sources: Nigeria (98 MtCO₂) > Tanzania (77 MtCO₂) > Ethiopia (56
624 MtCO₂).

625 In the fourth approach where we use the corrections of Grassi et al. (2022) except for DRC where we
626 kept the latest national communication instead of the most recent NDC, the continent is a net sink of -
627 504 MtCO₂ yr⁻¹ over 2001-2018. At regional scale, Central Africa is a large CO₂ sink, and the ranking
628 of sink regions is: Central African group (-620 MtCO₂ yr⁻¹) > North Africa (-259 MtCO₂ yr⁻¹) > South
629 Africa (-23 MtCO₂ yr⁻¹). The ranking of the source regions stays unchanged. At the country scale, the
630 main sink is DRC (-235 MtCO₂ yr⁻¹). In the paper, we will mainly use data corrected following Grassi et
631 al. (2022), but we want to raise a caution flag that adopting their correction for DRC had an enormous
632 effect on the CO₂ budget of the continent, which becomes a source. Using the original latest national
633 communication of DRC instead of the NDC used by Grassi et al., and our own corrections for Namibia
634 and Nigeria instead of those of Grassi et al. increased the continental CO₂ uptake.

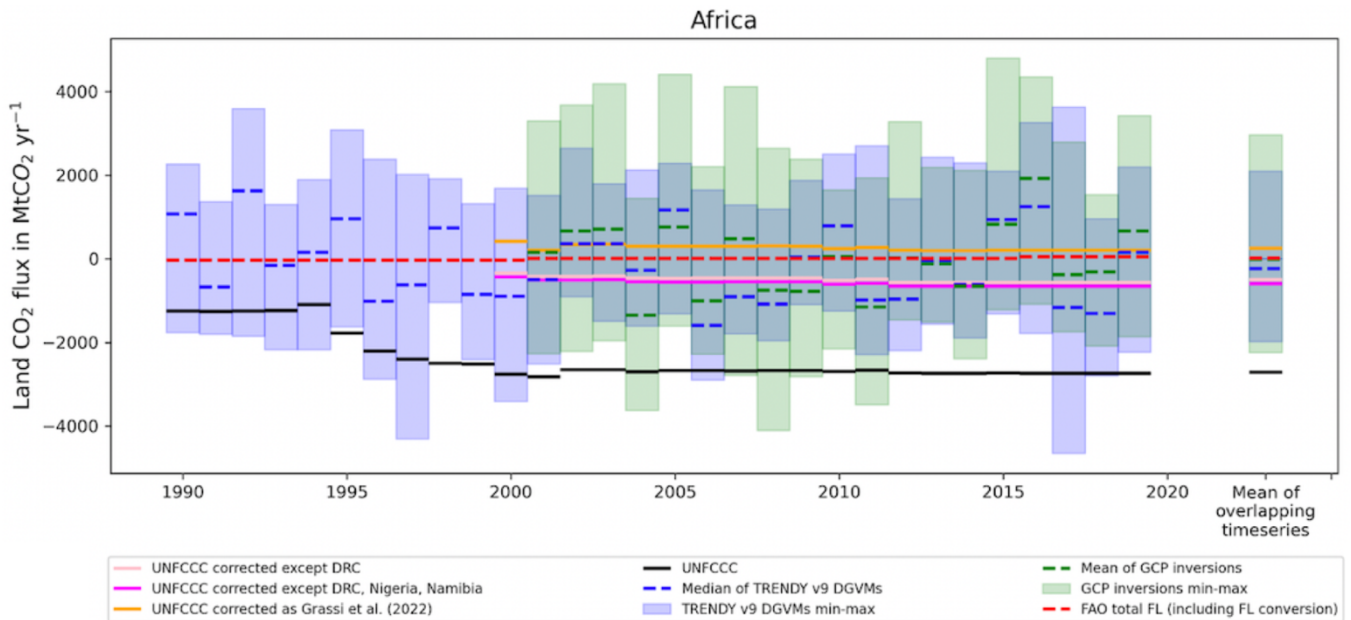
635

636 **Comparison of UNFCCC managed land area and FAO forest and other wooded lands areas**

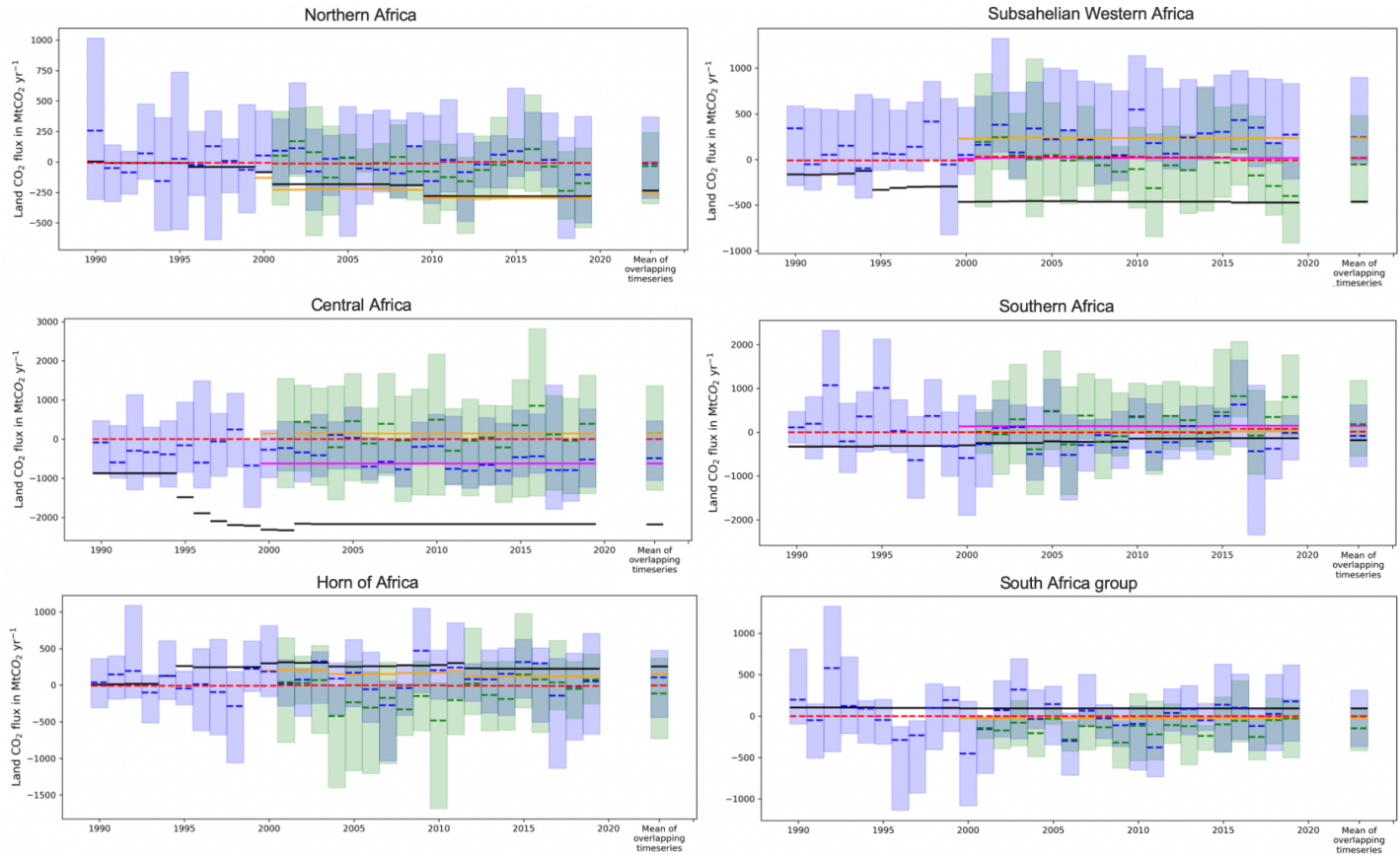
637 Figure S10 shows a comparison of land areas reported in NC, BUR and REDD+ reports
638 (<https://redd.unfccc.int/submissions.html?mode=browse-bycountry>) with FAO forest land areas (2015)
639 and FAO forest land + other woodlands areas for the year 2015 (see Table S9). Consistent with Grassi
640 et al. (2022), all forest lands in Africa are considered as managed. We found that FAO forest lands areas
641 are closer to UNFCCC estimates than the sum of FAO forest and other woodlands area, except for DRC,
642 Sudan, Senegal, Niger and Mauritania (Table S9). Forest areas in UNFCCC data using IPCC default
643 method do not exactly match FAO data estimates of forest area.
644

645 **LULUCF CO₂ fluxes from UNFCCC versus DGVM and inversions**

646 A comparison between LULUCF CO₂ fluxes from UNFCCC, FAO, DGVMs and inversions is shown
647 in Fig. 5 at the scale of the continent and for the six regions. The period of overlapping time series is
648 2001-2018. For the continent, DGVMs give a mean sink of -232 MtCO₂ yr⁻¹ with a huge range from -
649 1977 MtCO₂ yr⁻¹ to 2095 MtCO₂ yr⁻¹. The years with the biggest sinks for DGVM (from the median of
650 all models) are 2006 and 2018, and the years with the smallest sinks are 2005 and 2016 which seem
651 related to widespread drought years across Africa. A key result shown by this figure is that the DGVMs
652 and inversions show a huge spread, making them of little value to ‘verify’ inventories for LULUCF
653 CO₂ fluxes in Africa. Yet, we observed that the median of all DGVM points to a sink for Africa, unlike
654 the UNFCCC data with the correction from Grassi et al. (2022).



655



656
 657 **Figure 5. LULUCF CO₂ emissions and sinks: comparison between UNFCCC national greenhouse gas**
 658 **inventories, TRENDYv9 DGVMs and inversions, for total Africa and for each of the six African sub regions;**
 659 **as well as country details for the three lain outliers. The unit is in MtCO₂ yr⁻¹ Shaded green areas represent the**
 660 **minimum and maximum ranges from inversions. Shaded blue represents the minimum and maximum ranges**
 661 **for TRENDYv9 DGVMs. Green dashes denote the mean of inversions, blue dashes denote the median of**
 662 **TRENDYv9 DGVMs, green dashes the median of inversions. Positive values represent a source while the**
 663 **negative values refer to a sink.**

664
 665 For three large countries, corrected UNFCCC values from Grassi et al. show a bigger discrepancy with other
 666 BU and TD methods than uncorrected ones (Fig. S9). In Namibia the corrected value gives a larger sink
 667 compared to other methods, while the uncorrected value is comparable. In DRC the corrected value which
 668 was a source seems a high overestimate compared to other methods, while the uncorrected UNFCCC value
 669 is close to median values from inversions, and to FAO. In Nigeria, the corrected value seems to be a high
 670 overestimation of a net source compared to other methods pointing to either a smaller source (FAO,
 671 inversions) or even a sink (DGVM).
 672

673 The data in Figure 5 show that most methods agree on a small net sink for African LULUCF CO₂ fluxes,
674 except for corrections following Grassi et al (2022). But disagreements exist among different methods.
675 Inversions give a smaller net sink (mean_{min}^{max}) of -14 $\frac{2\ 966}{-2\ 248}$ MtCO₂ yr⁻¹ than DGVMs (-232 $\frac{2095}{-1978}$ MtCO₂
676 yr⁻¹). The median value of inversions is nevertheless within the range of DGVMs. At the scale of Africa,
677 the inversions mean sink is ~12 times smaller than the median from DGVMs. The min-max range of
678 inversions (5216 MtCO₂ yr⁻¹) is larger than the range of the DGVMs by 17%. DGVM and inversions show
679 a positive temporal correlation coefficient (r = 0.7) for annual trends (linear fit to time series).
680 UNFCCC values with the fourth approach point out to a net sink (-503 MtCO₂ yr⁻¹), similar to the third
681 one. Corrected values as in Grassi et al. (2022) give a net source estimate of 265 MtCO₂ yr⁻¹. FAO net
682 emissions and removals represent a small net source (18 MtCO₂ yr⁻¹). Differences between FAO and
683 UNFCCC, as explained in Grassi et al. (2022), could be due to the fact that FAO estimates of CO₂ fluxes
684 for forest remaining forest can be set to zero in absence of any national stock change inventory (Table 3).
685

686 **Table 3. Mean net LULUCF CO₂ (emissions and removals) over the overlapping period of the different**
687 **datasets (2001-2018), in MtCO₂ yr⁻¹.**

Region	Corrected UNFCCC (Grassi et al. 2022) with and without DRC correction.	Corrected UNFCCC but DRC/ Nigeria/ Namibia	Median TRENDY v9	Max TREND Y v9	Min TREND Y v9	Mean GCB inv.	Max GCB inv.	Min GCB inv.	FAO total FL with FL conversion
South Africa group	-23	-23	-5	312	-368	-147	96	-418	-1
Horn of Africa	153	153	108	475	-439	-115	367	-729	-5
Southern Africa	14	141	-81	622	-785	182	1186	-548	13
North Africa	-259	-259	-13	369	-299	-34	240	-343	-9
Subsahelian West Africa	236	19	245	900	-49	-53	481	-479	21
Central Africa	144 (DRC with NDC2021) -620 (DRC with NC3)	-620	-490	461	-1051	152	1362	-1303	-1
Africa total	265 (DRC with NDC2021) -503 (DRC with NC3)	-589	-232	2095	-1978	-14	2967	-2249	-1

689 At a regional scale, we note some agreement between different BU approaches. First, for the South Africa
690 region, the mean of DGVM medians during the overlapping period 2001-2018 ($-5 \text{ MtCO}_2 \text{ yr}^{-1}$) and the
691 FAO estimate ($-1 \text{ MtCO}_2 \text{ yr}^{-1}$) are comparable and not too far from Grassi et al., 2022 ($-23 \text{ MtCO}_2 \text{ yr}^{-1}$).
692 Second, for North Africa, the DGVM median ($-13 \text{ MtCO}_2 \text{ yr}^{-1}$) and the FAO mean estimate over the same
693 period ($-9 \text{ MtCO}_2 \text{ yr}^{-1}$) are comparable. Finally, in Sub-Saharan West Africa, the DGVM ($236 \text{ MtCO}_2 \text{ yr}^{-1}$)
694 and UNFCCC corrected following Grassi et al., 2022 ($245 \text{ MtCO}_2 \text{ yr}^{-1}$) are also close to each other.

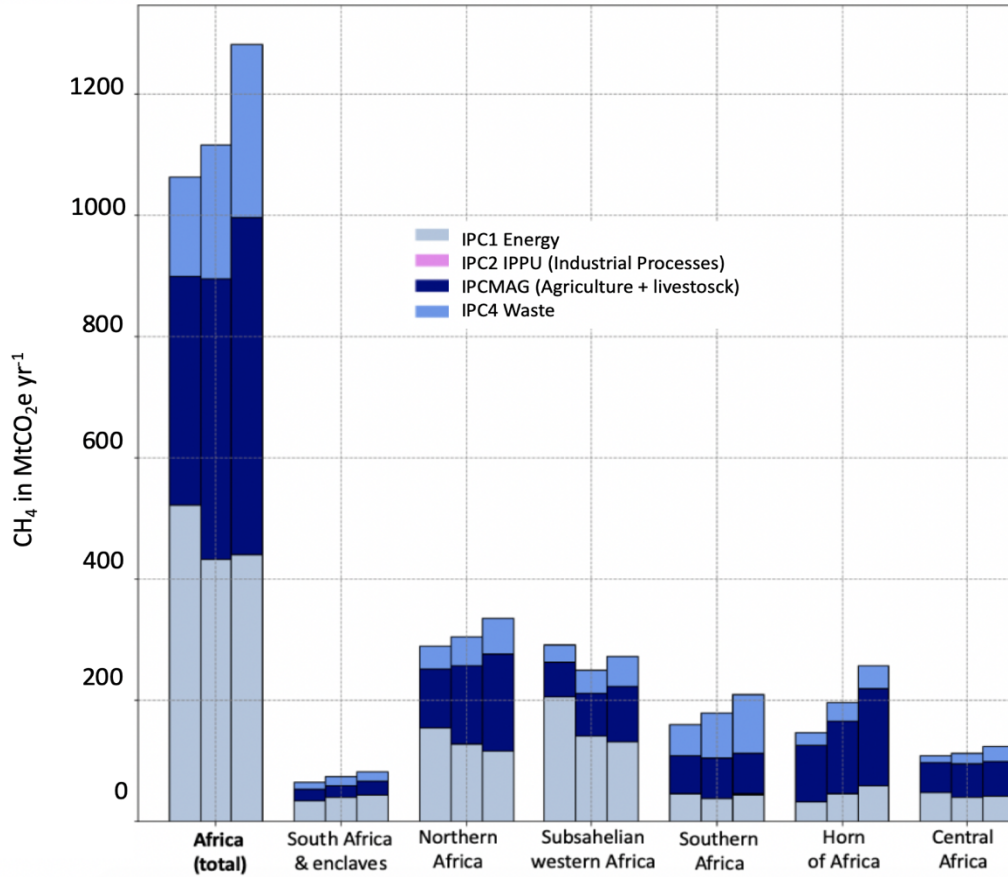
695
696 Northern Africa is the group where DGVM and inversions point to the closest values both in terms of sign
697 (sink) and magnitudes with respectively small sinks of $-13_{-299}^{369} \text{ MtCO}_2 \text{ yr}^{-1}$ and $-34_{-343}^{240} \text{ MtCO}_2 \text{ yr}^{-1}$.
698 Looking at DGVM and inversions in the region of South Africa, we found that both DGVM and inversions
699 point to a sink (respectively $-5_{-368}^{312} \text{ MtCO}_2 \text{ yr}^{-1}$ and $-147_{-418}^{96} \text{ MtCO}_2 \text{ yr}^{-1}$), however with a different
700 magnitude. The region showing the highest discrepancies between inversions and DGVM values is Central
701 Africa with a source in inversions ($152_{-1303}^{1362} \text{ MtCO}_2 \text{ yr}^{-1}$) and a sink for DGVM ($-490_{-1051}^{461} \text{ MtCO}_2 \text{ yr}^{-1}$).
702 The Sub-Saharan West Africa also shows discrepancies in both sign and magnitude with $245_{-49}^{900} \text{ MtCO}_2$
703 yr^{-1} for DGVM and $-53_{-479}^{481} \text{ MtCO}_2 \text{ yr}^{-1}$ for inversions. The same is true for Southern Africa with
704 $-81_{-785}^{622} \text{ MtCO}_2 \text{ yr}^{-1}$ for DGVMs and $182_{-548}^{1186} \text{ MtCO}_2 \text{ yr}^{-1}$ for inversions, and the Horn of Africa
705 with $108_{-439}^{475} \text{ MtCO}_2 \text{ yr}^{-1}$ for DGVM and $-115_{-729}^{367} \text{ MtCO}_2 \text{ yr}^{-1}$ for inversions. At the regional scale, the
706 inversions systematically give smaller sinks than DGVMs in the regions of Central Africa, Sub-Saharan
707 West Africa and North Africa after 2010 (Fig. 5).

708
709 We also computed the coefficient of correlation at the regional level between DGVM and inversions trends
710 for each region. The highest correlation coefficients are in the South Africa region ($r = 0.7$), followed by
711 Northern Africa ($r = 0.6$) and in Southern Africa ($r = 0.5$). The lowest correlation coefficients are for the
712 group of Central African countries ($r = 0.3$), Sub-Saharan Western countries ($r = 0.2$) and the Horn of
713 Africa ($r = 0.1$).

715 2.3 CH₄ anthropogenic emissions

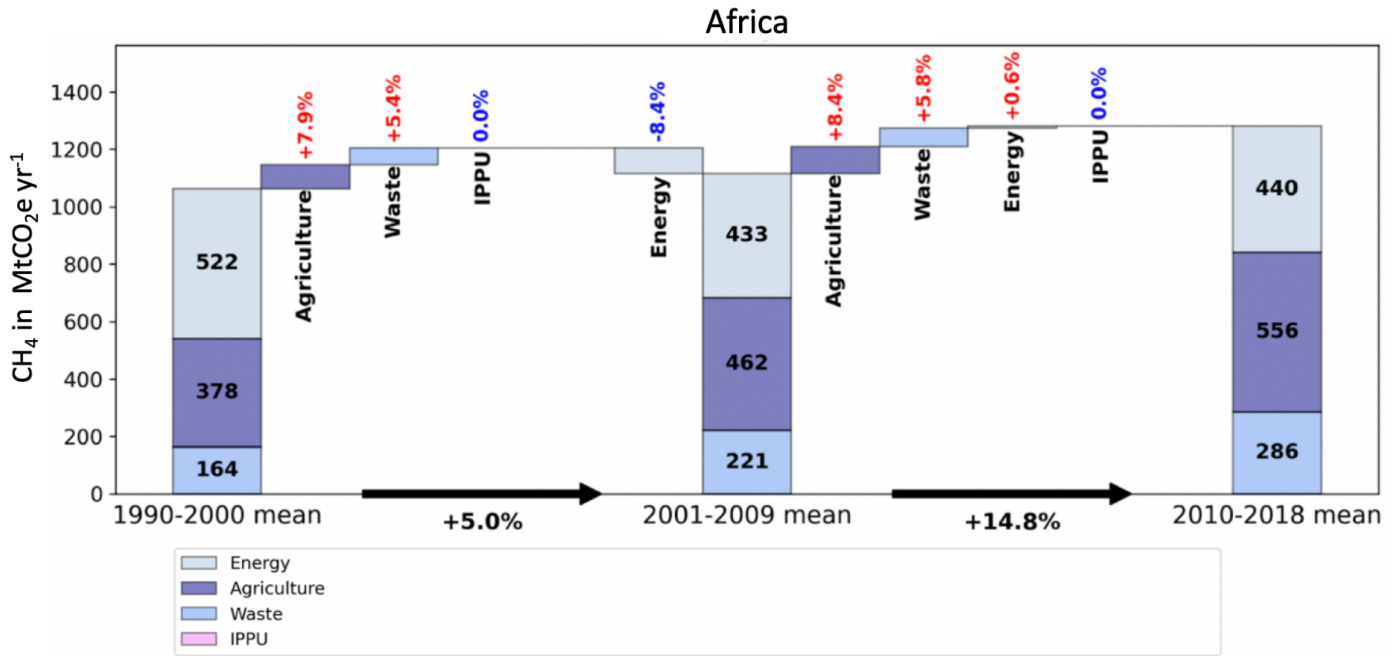
716 Total and sectoral bottom up CH₄ anthropogenic emissions and decadal changes

721 (a)



722

723 (b)



724

(c)

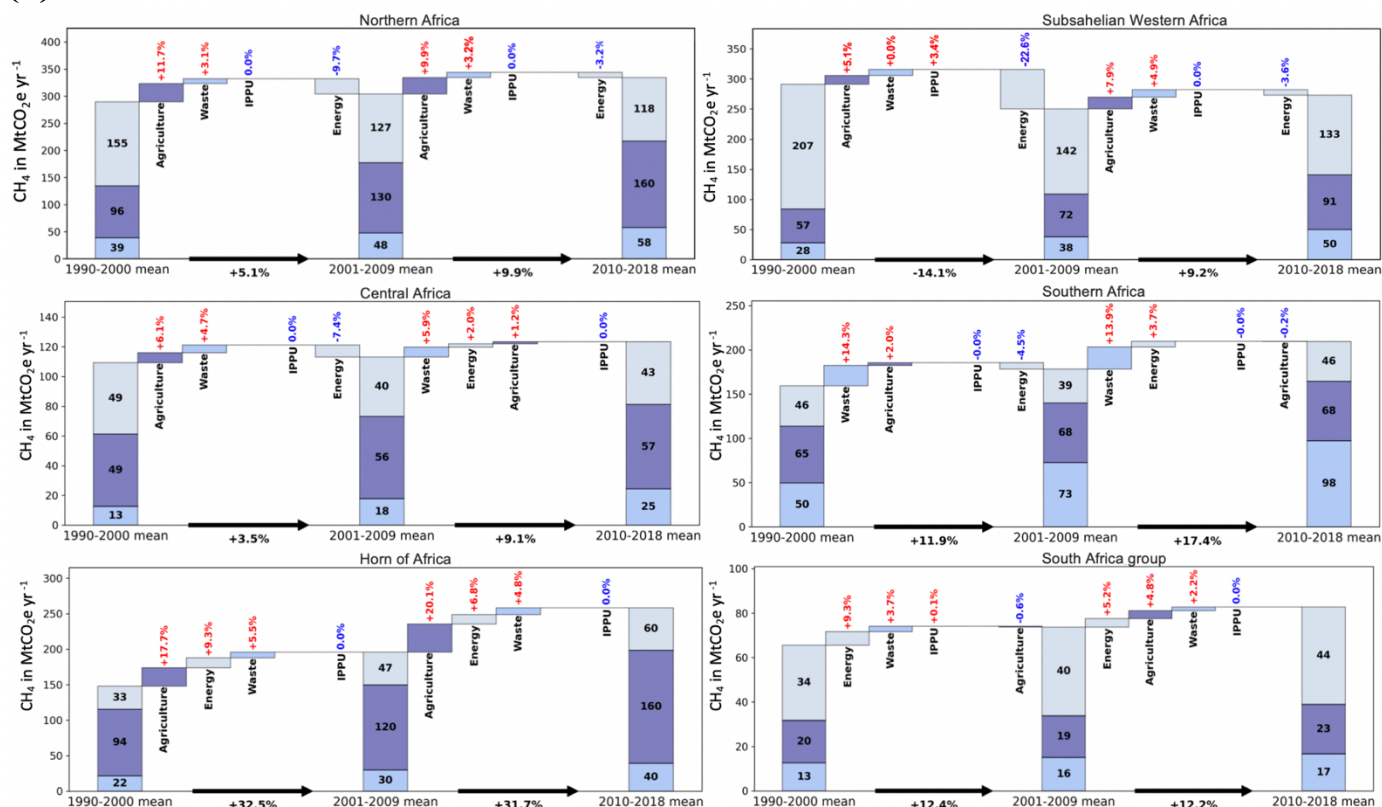


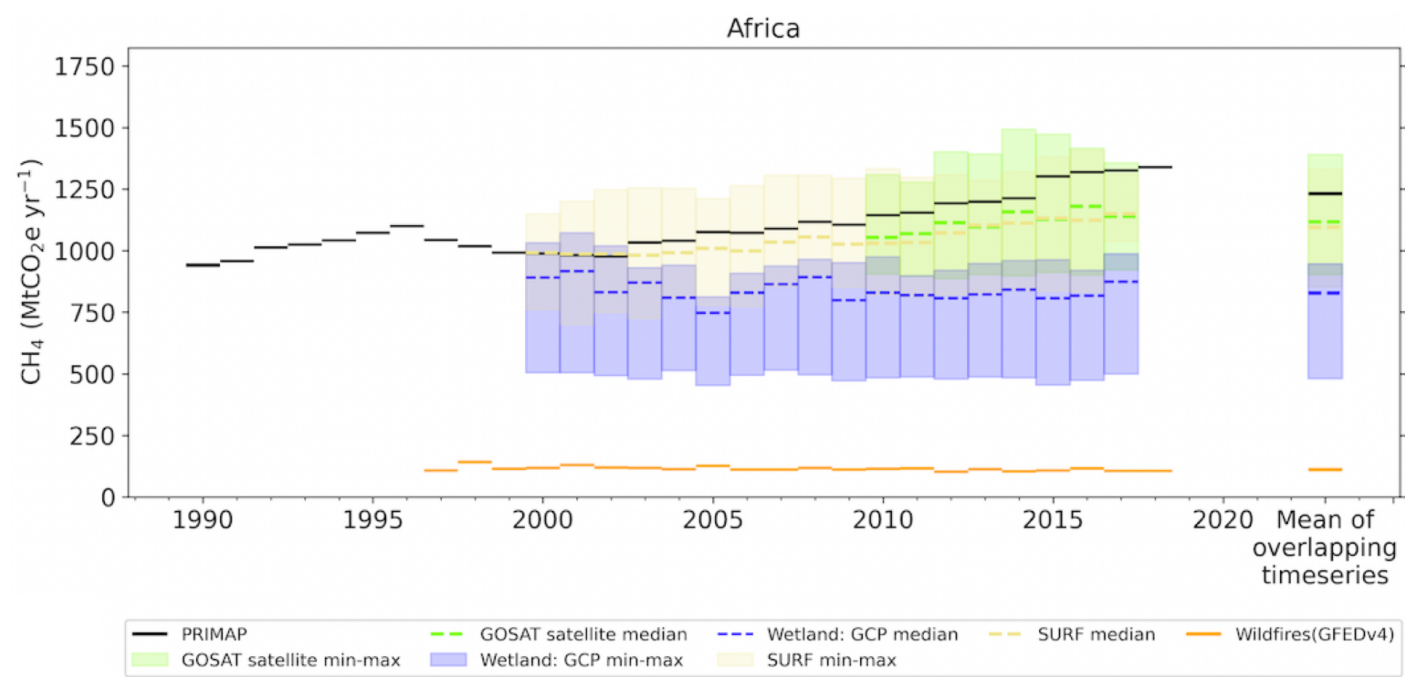
Figure 6. (a) African mean anthropogenic CH₄ emissions in MtCO₂e yr⁻¹ over three decades (1990-1998, 1999-2008, 2010-2018). (b) Contribution of each sector to the change of African emissions between the last three decades. (c) Same for different regions regrouping several countries. Data from PRIMAP-hist (2021).

Figure 6 shows anthropogenic CH₄ emissions from PRIMAP-hist grouped into four super-sectors (see section 1). A map of CH₄ emissions and their trends per country is given in Fig. 3c-d. LULUCF CH₄ emissions are not considered in PRIMAP-hist. African anthropogenic CH₄ emissions sum up to 1154 MtCO₂e yr⁻¹ over the last three decades. They increased from 1064 MtCO₂e yr⁻¹ in 1990-2000 to 1116 MtCO₂e yr⁻¹ in 2001-2009, and further to 1282 MtCO₂e yr⁻¹ over 2010-2018 (Fig. 6.a). Over the last three decades, the main African CH₄ emitting super-sectors shifted from Energy (49% over 1990-2000) to Agriculture, mainly due to a North African contribution. At the regional level, the main contributing region to total emissions shifted over the last 30 years from Sub-Saharan Western Africa (297 MtCO₂e yr⁻¹ for all sectors in 1990-2000) to North Africa (333 MtCO₂e yr⁻¹ for all sectors in 2010-2018).

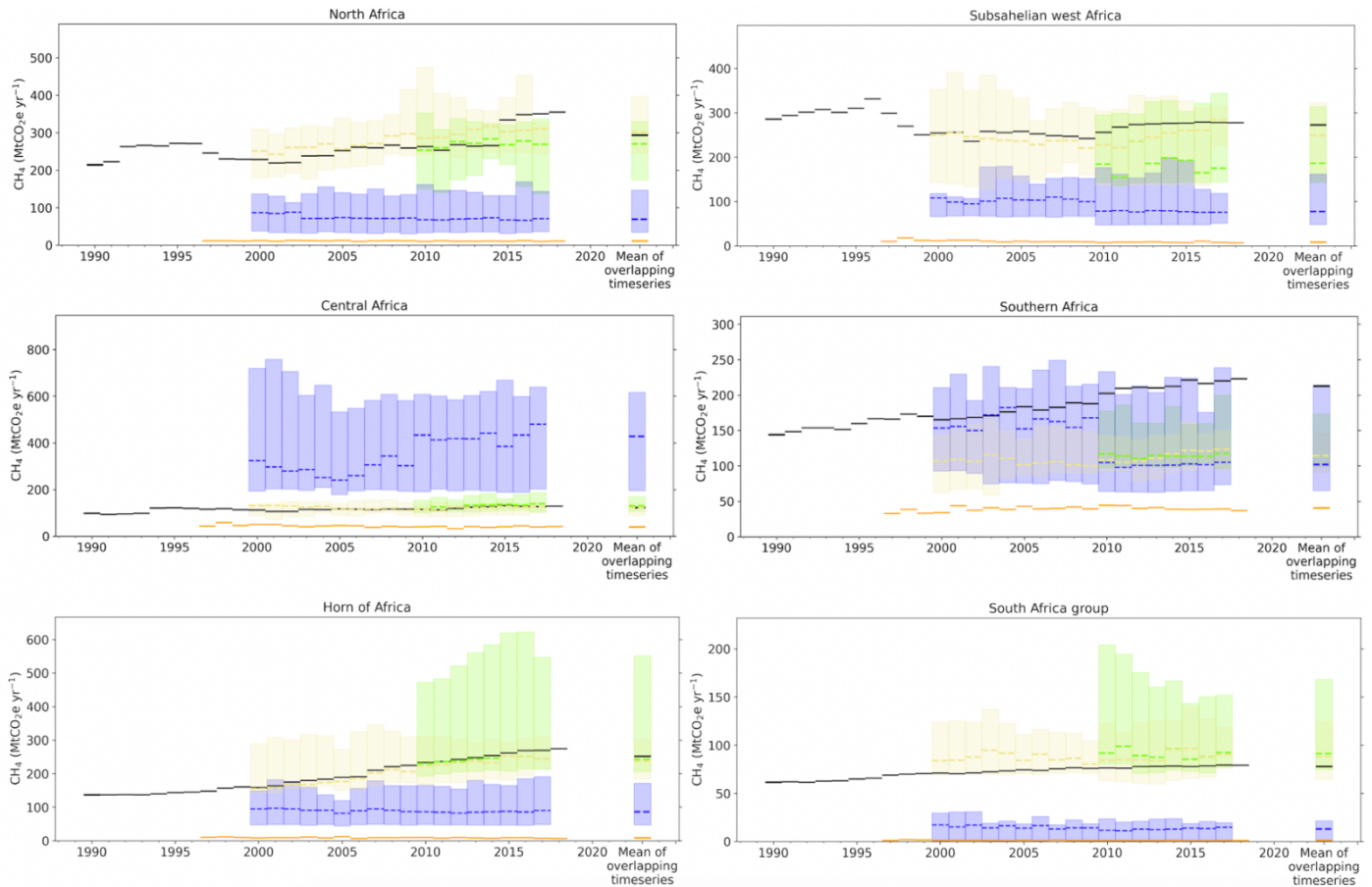
North African emissions increased from 290 MtCO₂e yr⁻¹ in 1990-2000 to 305 MtCO₂e yr⁻¹ in 2001-2009, and further to 333 MtCO₂e yr⁻¹ in 2010-2018. Sub-Saharan emissions decreased from 297 MtCO₂e yr⁻¹ in 1990-2000 to 252 MtCO₂e yr⁻¹ in 2001-2009, and re-increased to 274 MtCO₂e yr⁻¹ in 2010-2018, a level smaller than in the first decade (Fig. 6b). The Horn of Africa emissions increased from 149 MtCO₂e yr⁻¹ over 1990-2000, to

744 197 MtCO₂e yr⁻¹ over 2001-2009, and further to 260 MtCO₂e yr⁻¹ over 2010-2018. The emissions from Southern
 745 Africa increased from 184 MtCO₂e yr⁻¹ in 1990-2000, to 180 MtCO₂e yr⁻¹ in 2001-2009, and further to 212
 746 MtCO₂e yr⁻¹ in 2010-2018. Emissions from the Central African region increased from 111 MtCO₂e yr⁻¹ in 1990-
 747 2000, to 114 MtCO₂e yr⁻¹ in 2001-2009, and further to 125 MtCO₂e yr⁻¹ in 2010-2018. We also computed the
 748 GINI of African countries anthropogenic CH₄ per capita emissions and obtained the following values: 0.6 in
 749 1990-1998, 0.5 in 1999-2008, 0.5 in 2009-2018, thus a trend of increasing ‘inequality’ between countries. As
 750 compared to per capita FCO₂ emissions, more homogeneity is observed for CH₄ per capita emissions. Similar
 751 to FCO₂ emissions, the GINI values remained stable over the three decades, showing a similar level of
 752 inequalities over time.

753 **BU versus inversions for total and anthropogenic CH₄ emissions**



754



755
756
757
758
759
760
761
762
763
764
765
766
767
768
769
770
771

Figure 7. Comparison of total anthropogenic CH₄ emissions in MtCO₂e yr⁻¹ from the PRIMAP-hist inventory (black) and global inversions. Shaded green and yellow areas represent the minimum and maximum range from GOSAT satellite and surface inversions, respectively. Shaded blue areas represent the minimum and maximum ranges of wetlands natural emissions from inversions. The orange lines represent wildfire emissions from GFED4.

Figure 7 compares BU anthropogenic emissions from PRIMAP-hist for the period 2000-2018 with inversions' anthropogenic emissions (see section 1). Wetlands natural emissions are shown in the figure only for information from the median and range of inversions. Over the overlapping time period, medians of both GOSAT and surface inversions are always smaller than PRIMAP-hist emissions, at continental and regional level, except for the Central African region. For the African continent, the mean and min-max of GOSAT inversions for anthropogenic CH₄ emissions over 2000-2018 is 1117_{903}^{1390} MtCO₂e yr⁻¹, very close to the mean of surface inversions of 1094_{853}^{1330} MtCO₂e yr⁻¹. A good agreement between GOSAT and surface inversions was also found in other high-emitting countries (Deng et al., 2021). In contrast, PRIMAP-hist gives a mean of CH₄ anthropogenic emissions of 1231 MtCO₂e yr⁻¹ over the period 2010-2017. The mean wetlands flux from inversions over 2010-2017 is of 827_{481}^{946} MtCO₂e yr⁻¹. Methane emissions from wildfires over Africa for the same period are less important, with a mean of 110 MtCO₂e yr⁻¹.

772 Regional emissions from PRIMAP-hist ranked in decreasing order are: North Africa (293 MtCO₂e yr⁻¹) > Sub-
 773 Sahelian west Africa (272 MtCO₂e yr⁻¹) > Horn of Africa (252 MtCO₂e yr⁻¹) > Southern Africa (212 MtCO₂e
 774 yr⁻¹) > Central Africa (123 MtCO₂e yr⁻¹) > South Africa (78 MtCO₂e yr⁻¹). For both GOSAT and surface
 775 inversions, the ranking of regions (Table S11) is almost the same for surface inversions and PRIMAP-hist, with
 776 the exception of Central Africa and Southern Africa.

777

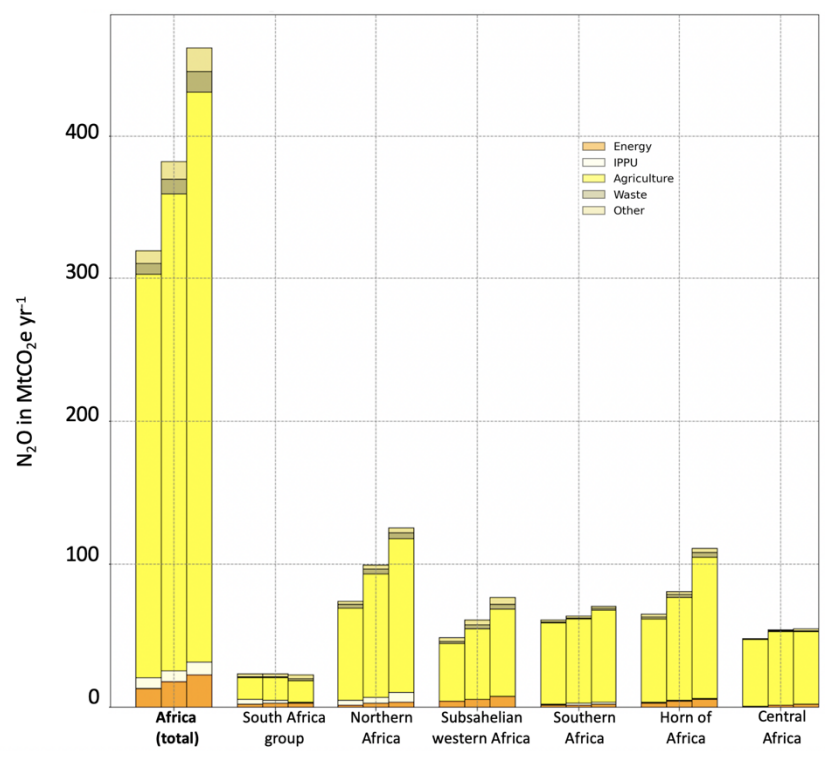
778 **2.4 Results for N₂O emissions**

779 **N₂O PRIMAP-hist versus atmospheric inversions (total flux)**

780 **Total and sectoral N₂O anthropogenic emissions (PRIMAP-hist)**

781

782 **(a)**



783

784

785

786

787

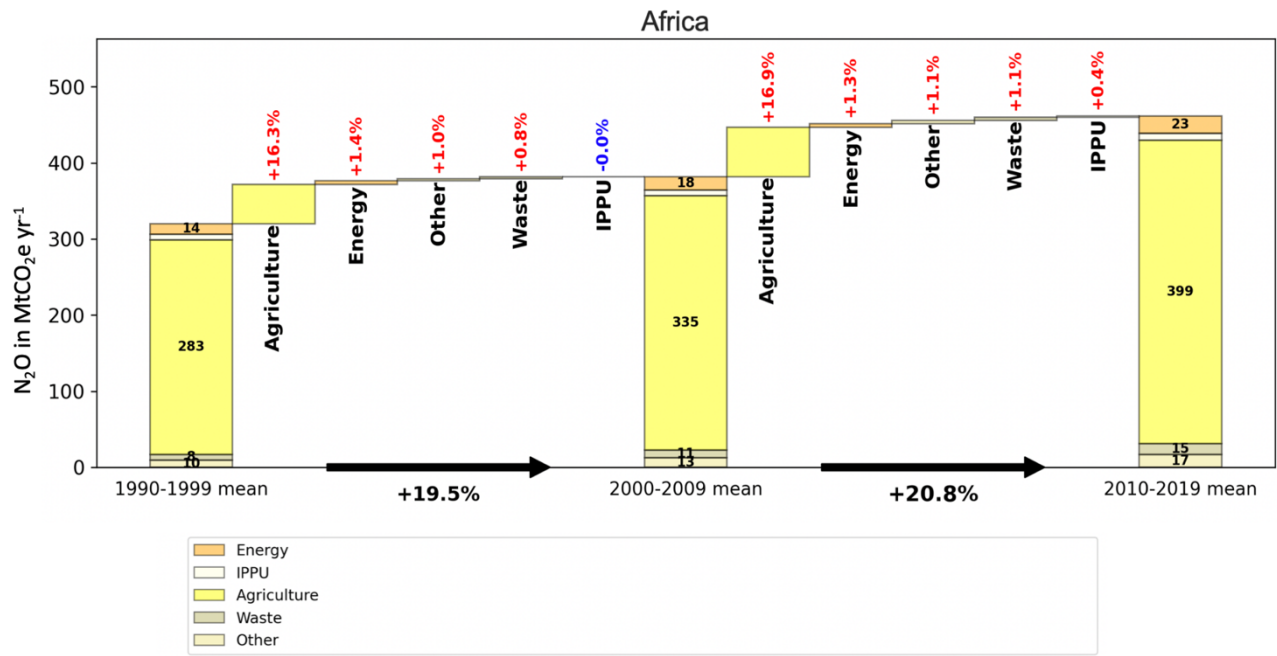
788

789

790

791

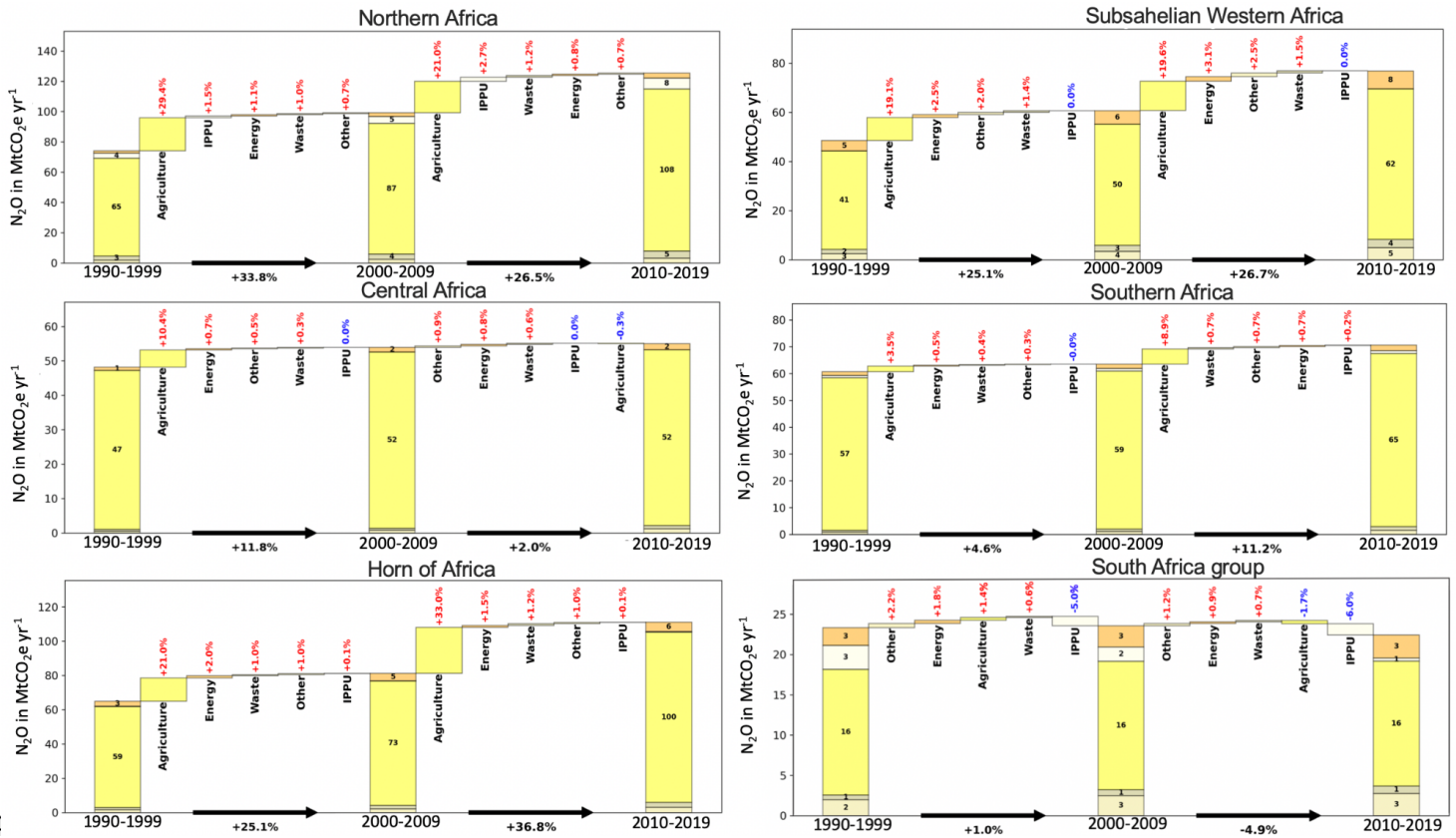
(b)



792

793

(c)

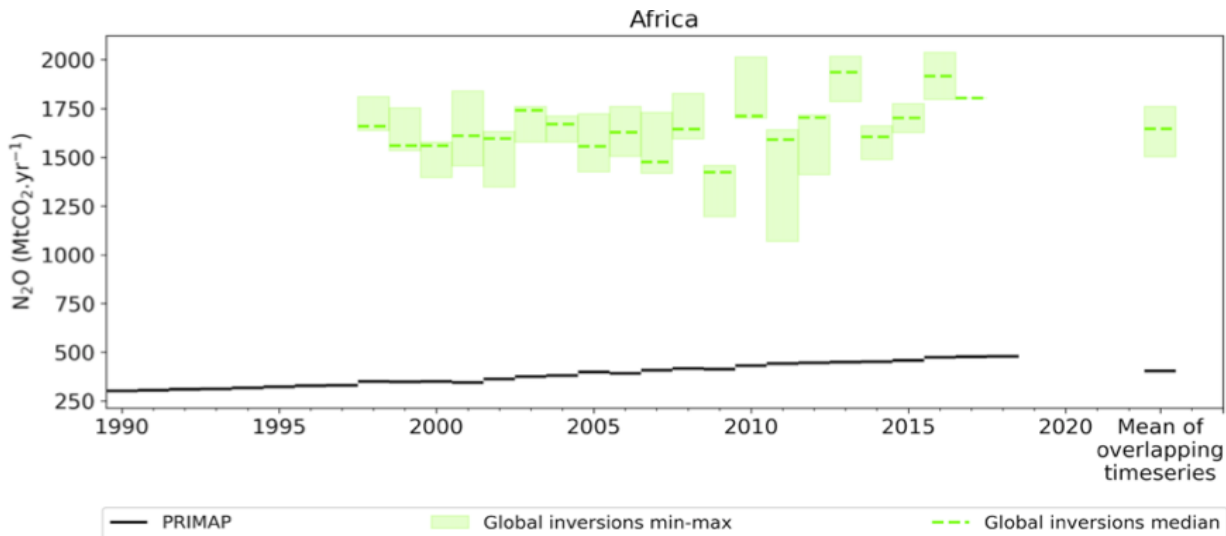


794

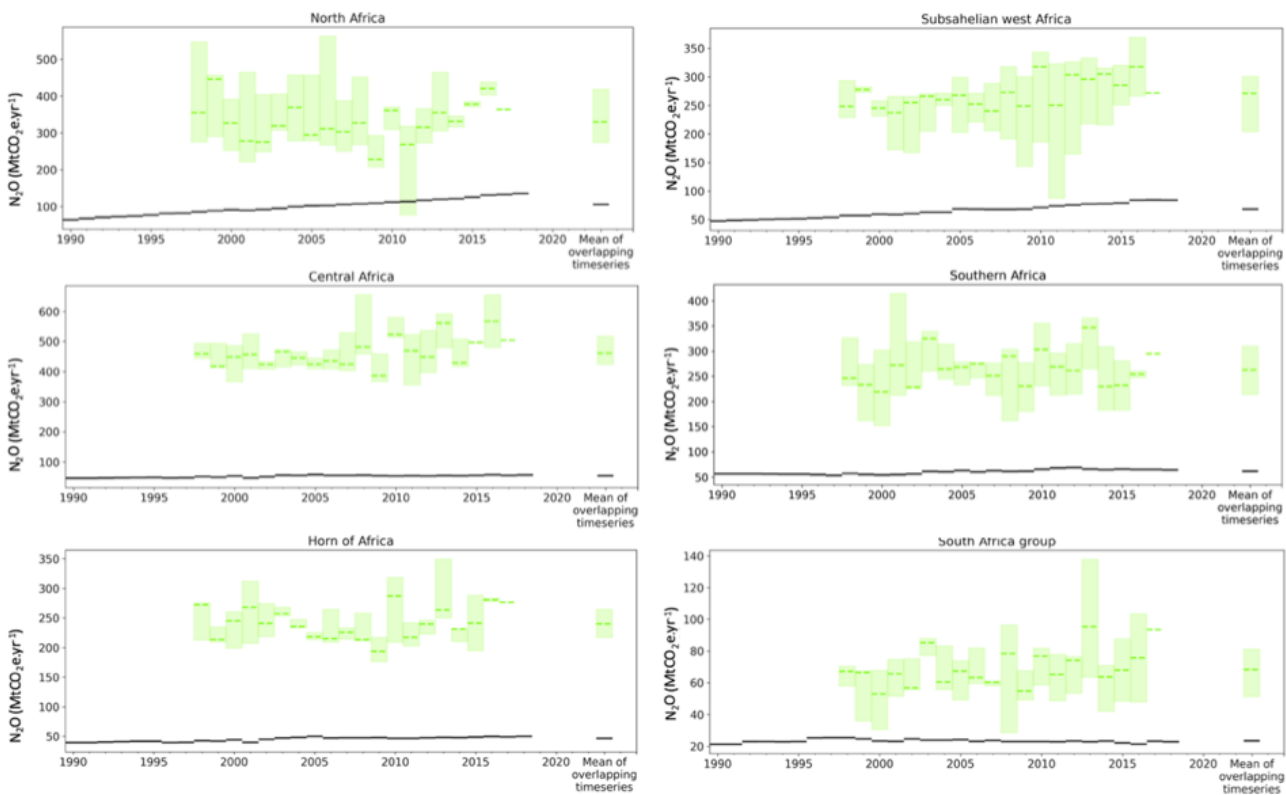
795 **Figure 8. (a) African anthropogenic N₂O emissions in MtCO₂e yr⁻¹ over three decades: 1990-1998, 1999-2008 &**
796 **2009-2019. Data from PRIMAP-hist (2021). (b) Contribution of each sector to the change of African N₂O emissions**
797 **between the last three decades. (c) Same for different regions regrouping several countries. Data from PRIMAP-**
798 **hist (2021).**

799 Figure 8 presents anthropogenic N₂O emissions from PRIMAP-hist, for five sectors (for country values, see
800 Fig. 4). Over the last three decades, the mean African emissions are 378 MtCO₂e yr⁻¹, three times less than CH₄
801 emissions. The mean decadal N₂O emissions increased from 319 MtCO₂e yr⁻¹ in 1990-1999, to 382 MtCO₂e yr⁻¹
802 ¹ in 2000-2009 (+20%), and further to 431 MtCO₂e yr⁻¹ in 2010-2018. Over the last three decades, the main
803 emitting sector remained Agriculture. The N₂O emissions increase also originates from Agriculture, with an
804 increase from 283 MtCO₂e yr⁻¹ to 335 MtCO₂e yr⁻¹ between 1990-1999 and 2000-2009, that is, +16.3 %
805 compared to of the total emission increase of +19.5%. The three other sectors show a smaller contribution to
806 the emissions increase: Energy (+1.4%), Other (+1%) and Waste (+0.8%). IPPU shows no change. Similarly,
807 between 2000-2009 and 2010-2019, the N₂O emissions increase also came from the sector of Agriculture, with
808 an increase from 335 MtCO₂e yr⁻¹ to 399 MtCO₂e yr⁻¹ between 1990-1999 and 2000-2009.

809 The main contributing regions to the continental emissions are Northern Africa and the Horn of Africa (Fig.
810 8a). Between 2000-2009 and 2010-2019, the North African contribution increased from 99 MtCO₂e yr⁻¹ to 125
811 MtCO₂e yr⁻¹ (+27%). The main sectoral contribution is always Agriculture, which increased in that region from
812 86 MtCO₂e yr⁻¹ to 107 MtCO₂e yr⁻¹ (+21%). Emissions from the second largest emitting region, the Horn of
813 Africa, increased from 81.19 MtCO₂e yr⁻¹ in 2000-2009 to 111 MtCO₂e yr⁻¹ in 2010-2019 (+37%), mainly from
814 Agriculture. In the third most emitting region, Sub-Saharan Africa, emissions increased from 61 MtCO₂e yr⁻¹
815 in 2000-2009 to 77 MtCO₂e yr⁻¹ in 2010-2019 (+27%), also from Agriculture. The least contributing region to
816 the increase of the total N₂O emissions from 2000-2009 to 2010-2019 is South Africa which had a very small
817 decrease, mainly from IPPU (-6%) followed by Agriculture (-2%). On the contrary, there is a slight increase of
818 N₂O emissions for the group of South Africa for the Other (+1%), Energy (+1%) and Waste (+1%) sectors.



819



820

821 **Figure 9. Total N₂O emissions from PRIMAP-hist in MtCO₂e yr⁻¹ (black line) from three GCP atmospheric**
 822 **inversions for the entire African continent and for six African sub-regions. The green line is the median of the three**
 823 **inversions and the light green areas the maximum-minimum range.**

824 Figure 9 compares N₂O emissions from PRIMAP-hist and inversions. For total Africa, the mean of inversions
 825 emissions over the overlapping time period 1998-2017 is $1647 \frac{1760}{1502}$ MtCO₂e yr⁻¹, much larger than the
 826 PRIMAP-hist estimate of 360 MtCO₂e yr⁻¹. According to PRIMAP-hist, total African emissions increased by

827 28% between 1998 and 2017, while the trend of emissions from the inversions is $16 \pm 8\%$. At regional scale,
828 emissions from inversions ranked in decreasing order are: Central Africa (461_{424}^{517} MtCO₂e yr⁻¹) >
829 North Africa (330_{274}^{419} MtCO₂e yr⁻¹) > Sub-Saharan West Africa (271_{68}^{330} MtCO₂e yr⁻¹) > Southern Africa
830 (263_{214}^{310} MtCO₂e yr⁻¹) > Horn of Africa (240_{217}^{265} MtCO₂e yr⁻¹) > South Africa (68_{51}^{81} MtCO₂e yr⁻¹). According to
831 PRIMAP-hist, the ranking is: North Africa (106 MtCO₂e yr⁻¹) > Sub-Saharan West Africa (68 MtCO₂e yr⁻¹) >
832 Southern Africa (62 MtCO₂e yr⁻¹) > Central Africa (54 MtCO₂e yr⁻¹) > the Horn of Africa (46 MtCO₂e yr⁻¹) >
833 South Africa (24 MtCO₂e yr⁻¹) (See also Table S13). Emissions from PRIMAP-hist are smaller than inversions
834 by a factor of 16. This is likely due to the fact that we did not attempt to separate natural from anthropogenic
835 emissions in inversions. Other studies (Ciais et al., 2021; Petrescu et al., 2021 in Europe) showed that even
836 after subtracting N₂O natural estimates, inversions always point to higher estimates than BU methods.

837

838 **3 Discussion: uncertainties, comparison between BU and TD methods, and synthesis for the three main** 839 **GHG**

840

841 **3.1 Uncertainties specific to DGVMs / inversions for LULUCF CO₂**

842

843 In Fig. 5, we showed important disagreements among models regarding LULUCF CO₂ on whether Africa has
844 been a small source over the last 20 years (as shown by inversions) or a net sink (as shown by DGVMs and
845 UNFCCC except with the Grassi et al. correction). There is also more interannual variability in the DGVMs
846 results, mainly from climate variability, which is absent from UNFCCC as inventories provide only decadal
847 smoothed flux estimates. The larger sink in the DGVMs compared to the corrected UNFCCC estimates using
848 the method of Grassi et al. (2022) may be due to the fact that non-Annex I UNFCCC estimates generally do
849 not include dead biomass or harvested wood products. If forest biomass is estimated by a stock-change
850 approach, therefore, changes in living biomass due to transfer to dead biomass and harvested wood products
851 will be considered emitted in that year, while in the DGVMs it will decay more slowly over time. Another
852 difference is the treatment of land use change emissions, based on historical global land use change maps for
853 the DGVMs, which can significantly differ from national land use datasets. On the other hand, DGVMs do not
854 represent forestry and may underestimate sinks in intensively managed young forests. DGVMs do not separate
855 between unmanaged and managed lands, while UNFCCC inventories only account for managed land, yet
856 including conservation areas and indigenous territories. Grassi et al. (2022) showed that the difference between
857 the global UNFCCC sink (1100 MtCO₂ yr⁻¹) and the global land carbon sink (4767 MtCO₂e yr⁻¹) must be
858 explained by the contribution of non-managed lands. But in the case of Africa, it was not possible to extract
859 from UNFCCC reports the national areas of unmanaged land, and we had to also look at UNFCCC Technical

860 Assessment Reports (TAR) as well as REDD+ reports to extract information. Methods of assessment have not
861 been fully standardized since 1990, and they differ depending on the countries analyzed, and on the emissions
862 categories considered. In this context, when comparing UNFCCC estimates with data from DGVM and
863 inversion models, different layers of aggregated uncertainties affect the analysis. (Deng et al., 2021; Petrescu
864 et al., 2021; Grassi et al., 2018). The fact that LULUCF CO₂ fluxes have the greatest uncertainties is true
865 globally.

866 **3.2 Differences and sources of uncertainties between BU and TD CH₄ emissions**

868 The methodology used for removing natural CH₄ emissions from inversions is key for comparing with BU
869 estimates of anthropogenic emissions only. In this paper, we used a separation based on the natural emissions
870 solved by each inversion (section 2.3 method 1). Using an alternative method from Deng et al. (2022) based on
871 natural emissions from the median of all inversions gives smaller anthropogenic emissions than PRIMAP-hist
872 (Fig. S10).

874 **3.3 Differences and sources of uncertainties between BU and TD N₂O emissions**

876 For N₂O emissions, discrepancies between inventories and inversions are very high, especially for the group of
877 Central African countries, where the vegetation covers an important land area with likely large natural N₂O
878 (Deng et al., 2022). We can suppose that more broadly for all African groups, the lack of accounting of natural
879 emissions is the main reason why PRIMAP-hist estimates are much smaller than inversions. All African
880 countries used Tier 1 emission factors and include only direct N₂O emissions. The study by Deng et al. (2022)
881 underlined that indirect anthropogenic emissions notably coming from “atmospheric nitrogen deposition and
882 leaching from anthropogenic nitrogen additions to aquifers and inland water are usually not reported by non-
883 Annex I countries” and that this under-reported source of anthropogenic emissions tends to represent about 5%
884 to 10% of anthropogenic N₂O. According to Deng et al. (2022), the global situation from inversions for main
885 emitters is similarly affected by the potential contribution of natural sources as well, which is difficult to
886 estimate and separate. Figure 11 from Deng et al. (2022) shows that even when removing “intact / non-managed
887 lands” from inversions, in many countries, especially tropical countries, the inversions give a systematically
888 much higher anthropogenic level of N₂O than inventories, suggesting that there are either missing
889 anthropogenic sources or some “natural” sources (e.g. conservation areas) in managed lands being
890 underestimated by inventories.

3.4 Synthesis of the steps for assessing net GHG trends over Africa

Here, we propose a first step towards the elaboration of what could become a more systematic method for a scientific benchmark of non-Annex I national inventories: 1) correct outliers, 2) check the plausibility of estimates, 3) have an independent evaluation of inventory data by experts, 4) a comparison between UNFCCC data corrected thanks to expert judgment and other BU and TD methods, 5) computation of the mean of all BU and TD methods, 6) computation of “best fitted BU values” (meaning “best fitted BU values” excluding uncorrected UNFCCC data), and “TD values” (meaning “best fitted TD values”: without considering N₂O inversions replaced with PRIMAP-hist values), 7) identification of ranking anomalies.

3.5 Net GHG budget from inversions

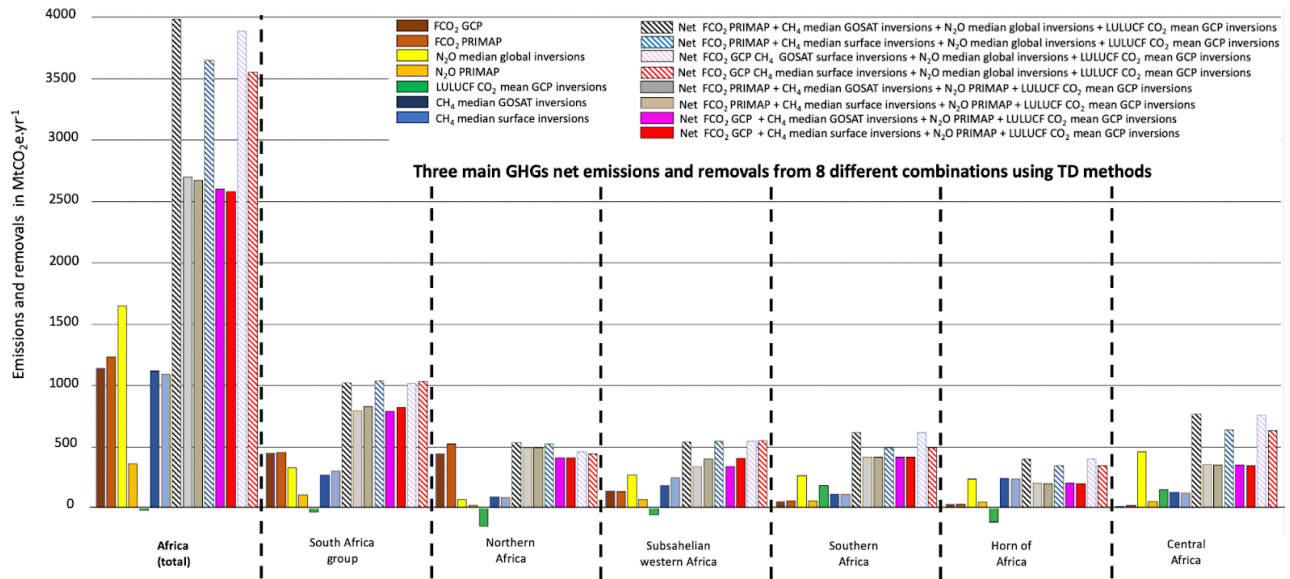
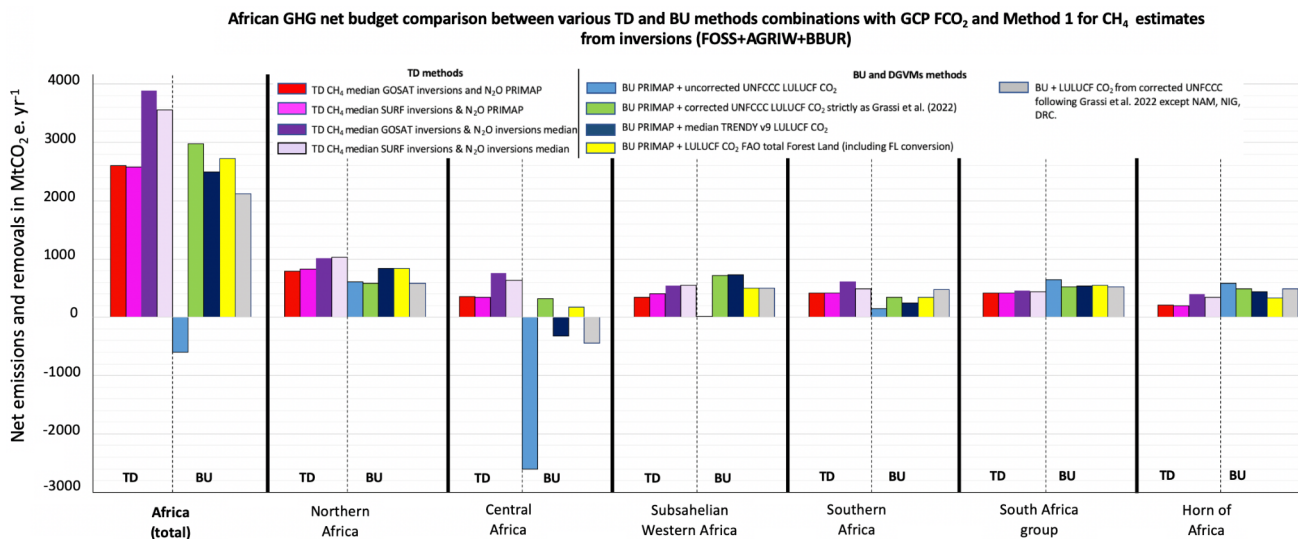


Figure 10. Synthesis for the three main GHG with net African budget computation by all TD methods for Africa as a whole and for six sub-groups of African countries across overlapping time series (2001–2017). Following the atmospheric convention, positive numbers represent an emission to the atmosphere and the negative values represent a sink. The CO₂ emissions and sinks from LULUCF are represented in green, they are taken from GCP 2020 dataset. Unit is MtCO₂e yr⁻¹.

Figure 10 shows different combinations of inversion GHG budgets and individual gasses contributions.

For total Africa, the mean net GHG budget from inversions where N₂O inversions are replaced by PRIMAP-hist is 2638_{1761}^{5873} MtCO₂e yr⁻¹. Regional GHG budgets in decreasing order are: North Africa (810_{279}^{1170} MtCO₂e yr⁻¹) > South Africa group (452_{161}^{751} MtCO₂e yr⁻¹) > Southern Africa (416_{334}^{1465} MtCO₂e yr⁻¹) > Sub-Saharan West Africa (373_{36}^{1051} MtCO₂e yr⁻¹) > Central Africa (352_{1133}^{1592} MtCO₂e yr⁻¹) > Horn of Africa

915 (204⁸⁷³₋₄₅₆ MtCO₂e yr⁻¹) (Table S17). The mean net of inversions including N₂O inversions is substantially
 916 higher, 3879⁷³⁴¹₁₃₂₀ MtCO₂e yr⁻¹. Regional GHG budgets in decreasing order are: North Africa
 917 (1034¹⁴⁷⁵₆₀₀ MtCO₂e yr⁻¹) > Central Africa (759²⁰⁵⁴₋₇₆₃ MtCO₂e yr⁻¹) > Southern Africa (616¹⁷¹³₋₂₆₂ MtCO₂e yr⁻¹) >
 918 Sub-Saharan West Africa (576¹³¹³₋₆₁ MtCO₂e yr⁻¹) > South Africa group (496⁸¹⁴₁₃₈ MtCO₂e yr⁻¹) (Table S17).
 919
 920 **3.6 Comparison between BU and TD methods**



921
 922
 923 **Figure 11. Synthesis for the three main GHG net African budget from TD and BU methods, using Method 1 for**
 924 **separating anthropogenic CH₄ emissions from inversions (FOSS+AGRIW+BBUR) during 2001-2017. FCO₂ data**
 925 **from GCP. N₂O from global inversions and from PRIMAP-hist. For TD methods, anthropogenic CH₄ from both**
 926 **GOSAT and surface inversions are used, and LULUCF from GCP inversions only. For BU methods, anthropogenic**
 927 **CH₄ and N₂O from PRIMAP are used, and with five different methods for assessing LULUCF CO₂: from**
 928 **uncorrected UNFCCC data; from corrected UNFCCC data according Grassi et al. (2022); from corrected**
 929 **UNFCCC except Namibia, Nigeria and DRC; from TRENDY v9; from FAO FL including FL conversions.**
 930 **Following the atmospheric convention, positive numbers represent an emission to the atmosphere and the negative**
 931 **values represent a sink. All values are in MtCO₂e.**

932
 933 Figure 11 shows the GHG budgets from all combinations of BU and TD methods. The mean of all methods
 934 after filtering outliers (Grassi et al. (2022) UNFCCC corrections, using PRIMAP instead of inversions for N₂O)
 935 is 2630⁴⁵⁵⁷₁₉₇₄ MtCO₂e yr⁻¹, which represents only 7.3 % of global FCO₂ emissions. The mean of all estimates
 936 points out to a source in the six African regions ranked in decreasing order as: North Africa (761⁹⁸⁸₄₆₀ MtCO₂e
 937 yr⁻¹ (513⁷⁰²₁₆₁ MtCO₂e yr⁻¹) > Horn of Africa (318⁶⁹⁹₋₈₀ MtCO₂e yr⁻¹) > Sub-Saharan West Africa
 938 (492⁹¹³₂₈₆ MtCO₂e yr⁻¹) > Southern Africa (354⁹⁹⁸₋₇₈ MtCO₂e yr⁻¹) > Central Africa (143⁸⁸²₋₆₇₀ MtCO₂e yr⁻¹).

939 We initially did not make any assumption regarding which approach is “better” between TD and BU method,
940 as it actually depends on the considered gas, sector and spatial scale. Comparability between TD and BU results
941 is not completely obvious either, as they do not represent the same processes (example of LULUCF CO₂ for
942 DGVM as explained in paragraph 3.1). For N₂O specifically, we highlighted in paragraph 3.3 the large
943 uncertainty of the TD estimates, underlining the importance to separate natural N₂O emissions from total
944 estimates in order to deliver appropriate anthropogenic assessments thanks to the inversions.

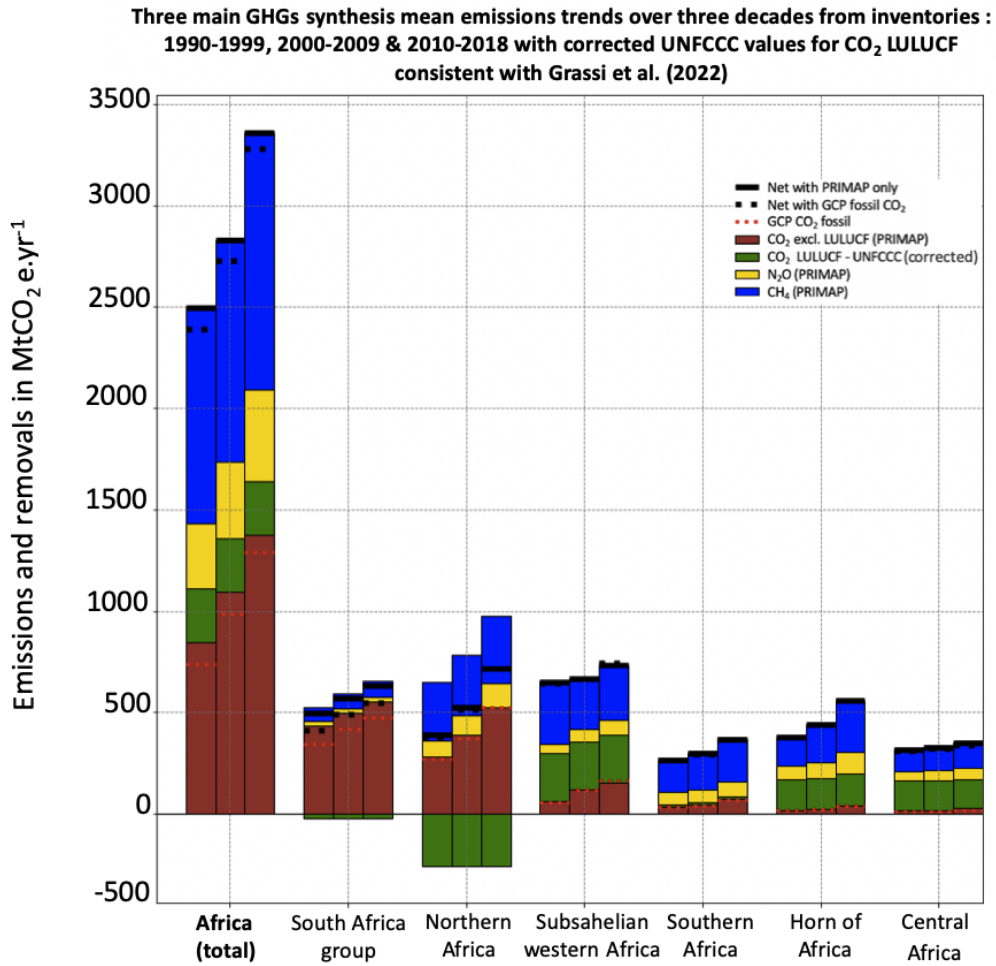
945

946 We showed in the results of this paper that inversions in general tend to have larger uncertainties than
947 inventories, and large differences in terms of min / max and at annual scale even among similar typologies of
948 the methods. But at a decadal scale, they deliver reliable overall trends (with good match among the median
949 values of various estimates on the overlapping time period) especially at the spatial scale of groups of countries
950 and of a continent. Under such conditions, TD estimates help identify or confirm outliers / large uncertainties
951 in inventories that may occur especially for Non-annex I countries like Africa.

952

953 Inversions therefore can't be a substitute but rather a complement to check trends consistency of inventories
954 and help to identify and correct main outliers. That's why we chose BU estimates to deliver a final budget over
955 Africa (with CO₂ LULUCF corrections) as synthesis figures (see Fig.12 and Fig.13 in the next paragraph).
956 Possibilities to reduce the gap BU and TD estimates are the following: 1) For inversions: to have a coarser
957 network of surface stations and coarser spatial resolution. 2) For DGVM: see paragraph 3.1. 3) For national
958 UNFCCC inventories: to have regularly updated activity data and use country-specific emissions data and
959 include indirect emissions, which is not the case to date for African countries, and use expert judgment for
960 correcting outliers as done by Grassi et al. (2022) and in this study for CO₂ LULUCF emissions.

3.7 Net GHG budget from BU estimates



962

963 **Figure 12. Synthesis for the three main GHG from inventories (after UNFCCC LULUCF CO₂ corrections**
 964 **consistent with Grassi et al. (2022)) for the three main GHG with net African budget computation by BU inventories**
 965 **for Africa as a whole and for six sub-groups of African countries across three different decades (1990-1999,**
 966 **2010, 2010-2018) using data and corrections from country inventories. Following the atmospheric convention,**
 967 **positive numbers represent an emission to the atmosphere and the negative values represent a sink. Black**
 968 **horizontal lines represent a net flux resulting from the addition of the three main GHG using PRIMAP-hist only,**
 969 **dashed black horizontal lines also represent the net flux resulting from the addition of the three main GHG but**
 970 **using the GCP dataset for FCO₂. Dashed red lines represent the fluxes from GCP FCO₂ available in the most recent**
 971 **GCP paper, to compare them with PRIMAP-hist results which are represented with the brown bar plots. The N₂O**
 972 **and CH₄ fluxes from PRIMAP-hist are respectively represented with yellow and blue bars. CO₂ emissions and**
 973 **sinks from LULUCF are represented in green, they are taken from NC/BUR UNFCCC datasets with corrections**
 974 **applied. Unit is MtCO₂e yr⁻¹.**

975

976 Figure 12 shows the budget for the three GHG from UNFCCC data with LULUCF data corrected using the
 977 second approach. There is a clear increase of African total GHG emissions during the last 3 decades. The
 978 differences between BU datasets are mainly due to different sectoral allocations. However, the trends are
 979 consistent and comparable, and differences among inventories tend to be less for the most recent decade.
 980

981 **Table 5. Mean net total Africa and regional groups' emissions and removals from BU methods using either GCP**
 982 **or PRIMAP-hist for FCO₂ over 2001-2017 in MtCO₂e.yr⁻¹.**

Region	Type of dataset									
	BU methods with GCP FCO ₂					BU methods with PRIMAP FCO ₂				
	GCP + uncorrected UNFCCC LULUCF CO ₂	GCP + corrected UNFCCC LULUCF CO ₂ as Grassi et al. (2022)	GCP + corrected UNFCCC LULUCF CO ₂ as Grassi et al. (2022) but for DRC, NAM, NIG	GCP + median TRENDY v9 LULUCF CO ₂ (min/max)	GCP + LULUCF CO ₂ total FL	PRIMAP + uncorrected UNFCCC LULUCF CO ₂	PRIMAP + corrected UNFCCC LULUCF CO ₂ as Grassi et al. (2022)	PRIMAP + corrected UNFCCC LULUCF CO ₂ as Grassi et al. (2022) but for DRC, NAM, NIG	PRIMAP + median TRENDY v9 LULUCF CO ₂ (min/max)	PRIMAP + LULUCF CO ₂ total FL
Africa total	-599	2975	2122	2478 ⁴⁸⁰⁶ ₇₃₂	2728	-502	3069	2216	2572 ⁴⁸⁹⁹ ₈₂₇	2822
North Africa	613	589	589	835 ¹²¹⁶ ₅₄₉	839	620	597	597	842 ¹²²⁴ ₅₅₇	846
Central Africa	-2605	316	-448	-318 ⁶³³ ₋₈₇₉	171	-2598	324	-440	-310 ⁶⁴¹ ₋₈₇₁	179
Subsahelian West Africa	19	718	501	726 ¹³⁸² ₄₃₃	503	15	714	497	723 ¹³⁷⁸ ₄₃₀	500
Southern Africa	149	346	473	251 ⁹⁵³ ₋₄₅₃	345	151	347	475	252 ⁹⁵⁵ ₋₄₅₂	346
South Africa group	640	524	524	542 ⁸⁶⁰ ₁₇₉	546	719	603	603	621 ⁹³⁹ ₂₅₈	625
Horn of Africa	586	484	484	438 ⁸⁰⁵ ₋₁₀₉	325	587	484	484	439 ⁸⁰⁶ ₋₁₀₈	326

983
 984 At the country level, a small number of countries showed an increasing difference between PRIMAP-hist and
 985 GCP estimates of fossil CO₂ emissions over time, but they are small FCO₂ emitters. The differences may also
 986 be partly explained by changes in accounting methods as mentioned in Gütschow et al. (2016). The biggest
 987 discrepancies are noticeable for Mali (64%), Cameroon (-62%), and the DRC (-38%), but those three countries
 988 are not major FCO₂ emitters (Fig. 4.a-b).

989 Table 5 shows the differences of net African budget from various BU methods using GCP or PRIMAP-hist for
 990 FCO₂ over 2001-2017 that are also illustrated on Fig. 11.

991 **BU LULUCF budget from UNFCCC corrected by Grassi (2022)**

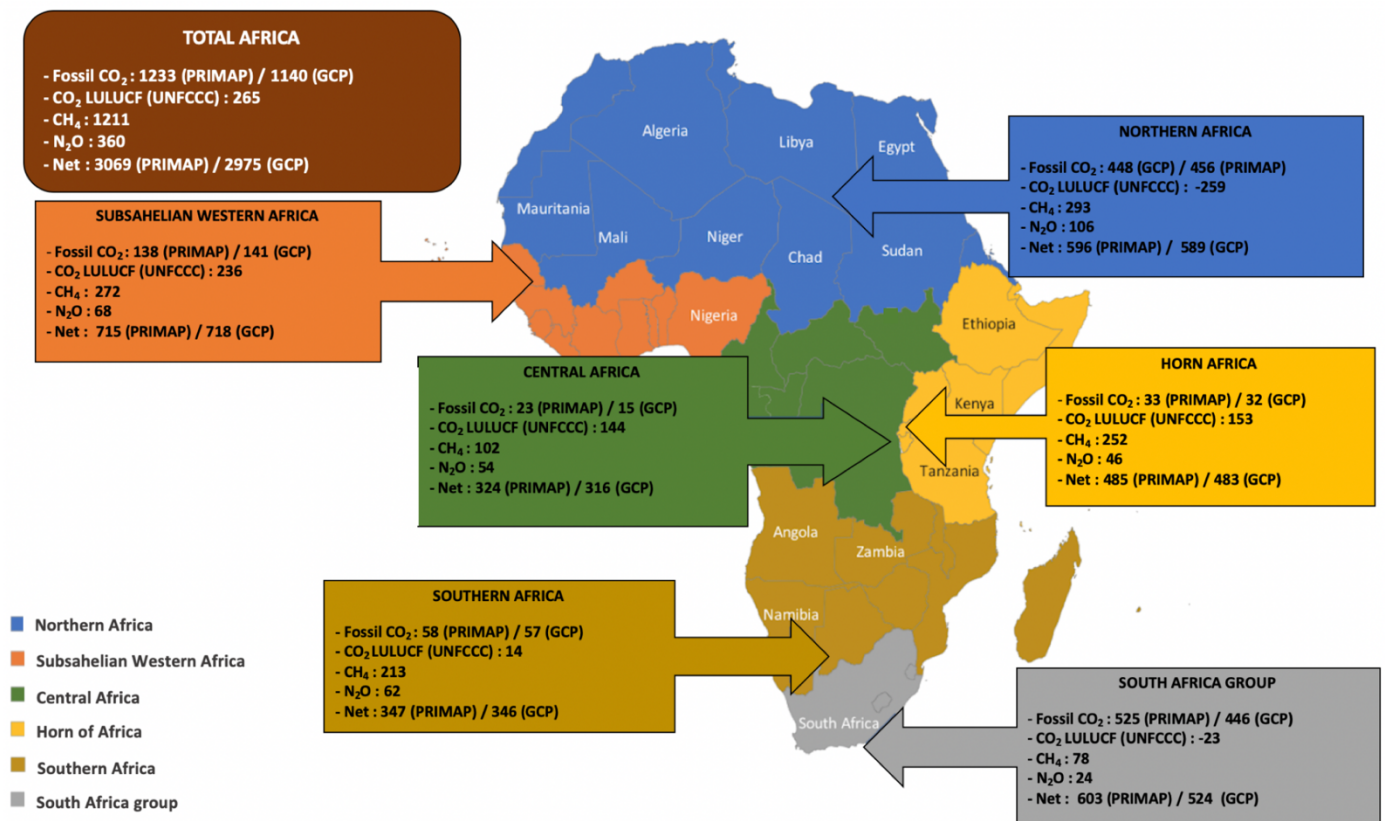
992 Over 2001-2017 the net BU GHG budget is 2975 MtCO₂e yr⁻¹. Regionally the ranking in decreasing order is:
 993 Sub-Saharan West Africa (718 MtCO₂e yr⁻¹) > North Africa (588 MtCO₂e yr⁻¹) > South Africa group (524
 994 MtCO₂e yr⁻¹) > Horn of Africa (484 MtCO₂e yr⁻¹) > Southern Africa (346 MtCO₂e yr⁻¹) > Central Africa (316
 995 MtCO₂e yr⁻¹).

996 **BU LULUCF budget CO₂ from FAO**

997 The BU budget from FAO data is 2728 MtCO₂e yr⁻¹, 8% less than above. The ranking of regions in decreasing
 998 order is: North Africa (838 MtCO₂e yr⁻¹) > South Africa group (546 MtCO₂e yr⁻¹) > Sub-Saharan West Africa
 999 (503 MtCO₂e yr⁻¹) > Southern Africa (345 MtCO₂e yr⁻¹) > Horn of Africa (325 MtCO₂e yr⁻¹) > Central Africa
 1000 (171 MtCO₂e yr⁻¹).

1001 **BU LULUCF budget from DGVMs**

1002 The net GHG budget for Africa is 2478⁴⁸⁰⁶₇₃₃ MtCO₂e yr⁻¹, 9% less than with FAO. The ranking of regions in
 1003 decreasing order is: North Africa (835¹²¹⁶₅₄₉ MtCO₂e yr⁻¹) > Sub-Saharan West Africa (726¹³⁸²₄₃₃ MtCO₂e yr⁻¹)
 1004 > South Africa (542⁸⁵⁹₁₇₉ MtCO₂e yr⁻¹) > Horn of Africa (438⁸⁰⁵₋₁₀₉ MtCO₂e yr⁻¹) > Southern Africa
 1005 (251⁹⁵³₋₄₅₃ MtCO₂e yr⁻¹) > Central Africa (-318⁶³³₋₈₇₉ MtCO₂e yr⁻¹).



1006

1007 **Figure 13. 2001-2018 emissions in MtCO₂e yr⁻¹ for fossil CO₂ (GCP and PRIMAP-hist), LULUCF CO₂ (corrected**
1008 **UNFCCC data consistent with Grassi et al. (2022), CH₄ (PRIMAP-hist), N₂O (PRIMAP-hist) for Africa, and for**
1009 **six regions.**

1010 For information, in the supplement section Fig. S13 and Fig. S14 illustrate the differences in MtCO₂e and in %
1011 for CH₄, N₂O and for the total net GHG budget that would result from the use of AR6 GWP100 compared to
1012 AR4 GWP100 currently in used by UNFCCC non-Annex I countries, for the six African regions considered on
1013 Fig.13 as well as for Africa total. The net difference on the total African budget for the use of GWP100 AR6
1014 instead of AR4 is: +4.6%, which means a relatively small increasing impact on the net budget, with a prevailing
1015 effect of the slight increase of CH₄ GWP100 in the AR6 as compared to AR4, over the strong decrease of N₂O
1016 GWP-100. The two African regions that are the most impacted in terms of net budget are: Southern Countries
1017 (+7.2%) and the Horn of Africa (+6.3%). The least impacted region in terms of overall net budget with an
1018 updated AR6 GWP-100 for CH₄ and N₂O is South Africa (+1.7%).

1020 **4 Summary, concluding remarks and perspectives**

1021 Africa is a large continent gathering 56 countries, and some countries are major GHG emitters. Because of its
1022 rapidly growing population and high industrial potential, Africa is a critical geography regarding climate
1023 change mitigation and adaptation policy. Depending on the emissions pathways, Africa, which is already a big
1024 emitting region, is expected to represent between at least a bit more than 10% of the global share by 2050, and
1025 could become as high as 18% of global emissions by 2050 (van der Zwaan, 2018).

1027 This paper delivers both a continental view and a detailed analysis of the three main GHG trends during the
1028 last thirty years across this continent as a whole, across relevant groups of countries given the inversions'
1029 resolutions, and also considering country details. Thanks to the comparison of different methods and datasets,
1030 the uncertainty about the net emissions and removals of GHG lowers. The interest of studying Africa is high
1031 not only from a scientific point of view, but also from a climate-policy perspective, as under the UNFCCC
1032 principle of “common but differentiated responsibility” about global warming, the credibility of the PA lies in
1033 the effective participation and inclusiveness of all parties, including non-Annex I countries. Our effort of
1034 comparing BU datasets and inversions and analyzing differences for African GHG emissions and removals
1035 assessment by looking at trends since 1990 will also be useful for future updates on a regular basis within the
1036 2023 GST perspective.

1037 At the scale of Africa, there is a rapid increase of FCO₂ emissions that roughly doubled since 1990. This increase
1038 is dominated by coal emissions for the decade 1990-1998 compared to 1999-2008 (+9%), and by oil for the

1039 decade 1999-2008 compared to the decade 2008-2017 (+16%). As for CO₂ LULUCF, we found that BU
1040 estimates are featured with important annual fluctuations, as opposed to periodic national inventories
1041 assessments, the reconciliation between the sectoral classification for anthropogenic estimates between TD and
1042 BU has to be done “manually” and is not uniform to date, which doesn’t facilitate the comparability of those
1043 different approaches. There are also differences among GCP inversions for CO₂, due to the fact that choices of
1044 model transport may differ among models, because prior fluxes can also differ between modeling teams, and
1045 because the African GHG observation network is featured with few stations and relatively scarce data. The lack
1046 of integration of CO₂ lateral anthropogenic and river fluxes is also an issue to be taken into account when trying
1047 to compare BU and TD methods (Ciais et al., 2022), and in the present study we did integrate those lateral
1048 fluxes. Anthropogenic CH₄ from PRIMAP-hist estimates indicate that out of the total African emissions
1049 increase from 1064 MtCO₂e yr⁻¹ to 1116 MtCO₂e yr⁻¹ between 1990-2000 and 2001-2009 (+5%), only two
1050 sectors contributed: Agriculture, in a dominant way (+8%) and Waste (+5%). Energy contributes to emissions
1051 decrease (-8%) that is however too small to offset other sectors’ CH₄ emissions that represent a net increase.
1052 The main regional contributions come from North Africa and from the Agriculture sector (+12%). Over the
1053 same period, the least contributing emitter is the group of South Africa (+12%), with only one decreasing
1054 emissions sector: Agriculture (-1%). The mean 2001-2009 emissions increased by +15% over 2010-2018 with
1055 contribution from all sectors except IPPU. This increase is dominated by Agriculture (+8%) and Waste (+ 6%).
1056 For 2010-2018, the two main contributing regions for CH₄ emissions are Northern Africa and Sub-Saharan
1057 Western Africa, Agriculture being the dominant emitting sector. From inversions, after withdrawing natural
1058 emissions and wildfires using the GFED dataset from total CH₄ emissions, median values are almost always
1059 below PRIMAP-hist estimates. CH₄ natural emissions have an important impact in Africa especially in the
1060 Central African region as well as in the Southern countries. N₂O TD estimates are always higher than the ones
1061 from PRIMAP-hist, underlining the importance to separate natural N₂O emissions from total estimates in order
1062 to deliver appropriate anthropogenic assessments thanks to the inversions.

1063 To compute a net budget for the three main GHG emissions and removals and for comparability we used the
1064 MtCO₂e yr⁻¹ metric and the latest IPCC report recommended GWP. The choice of a constructed GWP metric,
1065 however, creates additional associated uncertainties notably due to the selected time horizon. By computing
1066 the mean of methods excluding uncorrected UNFCCC and N₂O inversions data from twenty different ways for
1067 assessing GHG emissions and removals in Africa, we found that the most recent net from the three main GHG
1068 in Africa is a source of 2630^{4557}_{1974} MtCO₂e yr⁻¹.

1069 Our assessment of African GHG emissions trends over 30 years through different methods can enable
1070 comparisons of *ex post* with *ex ante* pledges of the PA, whose baseline year is often 1990. However, given the
1071 global geopolitics to date featured with the prevailing principle of national sovereignty, a scientific assessment

1072 of GHG can only work as a supporting tool (Janssens-Maenhout et al., 2020) and cannot be directly policy-
1073 prescriptive. We note a relatively good match among the various types of estimates in terms of overall trends,
1074 especially at a regional level and on a decadal basis, but large differences in terms of min / max and at annual
1075 scale even among similar typologies of the methods (TD or BU). The large discrepancies are a scientific limit
1076 to the possibility of precise verification of the African country-reported emissions, but they are good enough
1077 to indicate trends. To compute a net from the three main GHG, no purely “TD” method is available due to the
1078 necessity to replace N₂O inversions data with BU data. An original result of this study is that we proposed at a
1079 small scale what may become a systematic formalized methodological protocol for independent verification of
1080 a net estimate using country-reported data, to be possibly implemented at the UNFCCC secretariat scale in a
1081 centralized way. The African GHG increasing trend is not in line with the mitigation aims of the PA towards
1082 net-zero globally. Research teams focusing on inversion methods (Nickless et al., 2020), underline that
1083 uncertainties should not be above 15% in order to deliver a reasonable verification support capacity. A major
1084 source of complexity for the evaluation of the respect of the Paris Agreement comes from the fact that national
1085 pledges generally fall below the discrepancies between different scientific independent estimates. This calls for
1086 investments not only in improvements of atmospheric measurement devices but also in the research efforts for
1087 standardizing verification methods. At the policy level, the extrapolation of this study to the climate policy
1088 field could also serve as a compelling argument for the creation of a global dedicated “Climate Inspection task
1089 force” of the UNFCCC.

1090 **5 Data availability**

1091 The datasets from the three main greenhouse gasses used in this paper (CO₂, CH₄, N₂O) from the various BU
1092 inventories, TD inversions and DGVM over Africa will be made publicly available. This database is available
1093 from Zenodo at: <https://doi.org/10.5281/zenodo.7347077> (Mostefaoui et al., 2022).

1094 This dataset contains 32 data files:

1095 **- CO₂ inversions** (annual flux for LULUCF CO₂)

- 1096 - African CO₂ TD inversions GCB2020 1990-2019: annual CO₂ flux from GCB inversion models
- 1097 - African CO₂ lateral flux 2001-2019: annual CO₂ lateral flux including river transport, crop and wood
1098 product trade.
- 1099 - African CO₂ TRENDYv9 1990-2019: annual CO₂ flux from 14 DGVM
- 1100 - FAO 1990-2019: annual emissions and removals from FAO dataset
- 1101 - Inventory IPCC 1990-2019: annual flux from inventory data collected from UNFCCC national
1102 inventories in the IPCC categories

1103 **- CH₄ inversions 2000-2017** (annual flux)

1104 - African CH₄ global inversion 2000-2017: CH₄ flux over 2000-2017 from 11 surface inversion and 11
1105 satellite inversion models from four sectors; fossil refers to emissions from the fossil sector; agriculture and
1106 waste refers to emissions from both the agriculture and waste sector; biomass burning refers to emissions from
1107 biomass burning

1108 - GFEDv4 1997-2016: wildfire emissions from the Global Fires Emission Dataset (GFED) version 4

1109 - **N₂O inversions 1998-2017** (annual flux)

1110 - N₂O PYVAR 1998-2017: total N₂O emissions from PyVAR inversions;

1111 - N₂O TOMCAT-INVICAT 1998-2015: total N₂O emissions from TOMCAT-INVICAT model;

1112 - N₂O MIROC4 - ACTM 1998-2016: total N₂O emissions from MIROC4-ACTM model;

1113 Data used in this study are also included in the Supplementary Information (for example, from FAO data) and
1114 on public websites (CDIAC, PRIMAP-hist, World Bank data). Any other data that support the findings of this
1115 study are available from the corresponding author upon request.

1116
1117 **Author contributions.** MM, PC, PP and MJM designed research and led the discussions; MM wrote the initial
1118 draft of the paper and edited all the following versions; MM made all figures ; MJM and PP processed the
1119 original data from inversions and DGVM; MM processed the UNFCCC data and corrections; PC, PP and YE
1120 gave valuable suggestions to the manuscript structure; PC, MJM and PPP read, gave comments and advice on
1121 previous versions of the manuscript; all co-authors commented on specific parts related to their datasets; PC,
1122 MJM, PP, FC, SS, CR, IL, MS, PP are data providers.

1123 **Competing interests.** The authors declare that they have no conflict of interest.

1124
1125 **Disclaimer.** The views expressed in this publication are those of the authors.

1126 1127 **Acknowledgements**

1128 MM acknowledges funding from Sorbonne University, Institute of the Environmental Transition. PC, PP, and
1129 MJM were supported by the European Commission, Horizon 2020 Framework Program (VERIFY, grant no.
1130 776810). PC and YE are also supported by the RECCAP2 project (grant no. ESRIN/4000123002/18/I-NB).
1131 We acknowledge Stephen Sitch and Trendy modelers for the use of their dataset. We also acknowledge
1132 Christian Rödenbeck for the use of CarboScope, Frédéric Chevallier for CAMS, Ingrid Luijkx for CTE,
1133 Marielle Saunois for CH₄ inversions. The PyVAR-N₂O modeling results were provided by Rona Thompson
1134 (NILU) and were funded through the Copernicus Atmosphere Monitoring Service
1135 (<https://atmosphere.copernicus.eu/>), implemented by ECMWF on behalf of the European Commission, and
1136 were generated using computing resources from LSCE.

1137
1138
1139
1140
1141
1142
1143
1144
1145
1146
1147
1148
1149
1150
1151
1152
1153
1154
1155
1156
1157
1158
1159
1160
1161
1162
1163
1164
1165
1166
1167
1168
1169
1170
1171
1172
1173
1174
1175
1176
1177
1178
1179
1180
1181
1182
1183
1184

References

- Andrew, R. M.: A comparison of estimates of global carbon dioxide emissions from fossil carbon sources, *Earth Syst. Sci. Data*, 12, 1437–1465, <https://doi.org/10.5194/essd-12-1437-2020>, 2020.
- Ayompe, L. M., Davis, S. J., and Egoh, B. N.: Trends and drivers of African fossil fuel CO₂ emissions 1990–2017, *Environ. Res. Lett.*, 15, 124039, <https://doi.org/10.1088/1748-9326/abc64f>, 2020.
- BP. BP Statistical Review of World Energy, 2020.
- Beck, H. E., Zimmermann, N. E., McVicar, T. R., Vergopolan, N., Berg, A., and Wood, E. F.: Present and future Köppen-Geiger climate classification maps at 1-km resolution, *Sci. Data*, 5, 180214, <https://doi.org/10.1038/sdata.2018.214>, 2018.
- Bombelli, A., Henry, M., Castaldi, S., Adu-Bredu, S., Arneith, A., de Grandcourt, A., Grieco, E., Kutsch, W. L., Lehsten, V., Rasile, A., Reichstein, M., Tansey, K., Weber, U., and Valentini, R.: An outlook on the Sub-Saharan Africa carbon balance, *Biogeosciences*, 6, 2193–2205, <https://doi.org/10.5194/bg-6-2193-2009>, 2009.
- Canadell, J. G., Raupach, M. R., and Houghton, R. A.: Anthropogenic CO₂ emissions in Africa, *Biogeosciences*, 6, 463–468, <https://doi.org/10.5194/bg-6-463-2009>, 2009.
- Chevallier, F., Fisher, M., Peylin, P., Serrar, S., Bousquet, P., Bréon, F.-M., Chédin, A., and Ciais, P.: Inferring CO₂ sources and sinks from satellite observations: Method and application to TOVS data, *J. Geophys. Res. Atmospheres*, 110, <https://doi.org/10.1029/2005JD006390>, 2005.
- Ciais, P., Bastos, A., Chevallier, F., Lauerwald, R., Poulter, B., Canadell, J. G., Hugelius, G., Jackson, R. B., Jain, A., Jones, M., Kondo, M., Lujikx, I. T., Patra, P. K., Peters, W., Pongratz, J., Petrescu, A. M. R., Piao, S., Qiu, C., Von Randow, C., Regnier, P., Saunois, M., Scholes, R., Shvidenko, A., Tian, H., Yang, H., Wang, X., and Zheng, B.: Definitions and methods to estimate regional land carbon fluxes for the second phase of the REgional Carbon Cycle Assessment and Processes Project (RECCAP-2), *Geosci. Model Dev.*, 15, 1289–1316, <https://doi.org/10.5194/gmd-15-1289-2022>, 2022.
- Deng, Z., Ciais, P., Tzompa-Sosa, Z. A., Saunois, M., Qiu, C., Tan, C., Sun, T., Ke, P., Cui, Y., Tanaka, K., Lin, X., Thompson, R. L., Tian, H., Yao, Y., Huang, Y., Lauerwald, R., Jain, A. K., Xu, X., Bastos, A., Sitch, S., Palmer, P. I., Lauvaux, T., d’Aspremont, A., Giron, C., Benoit, A., Poulter, B., Chang, J., Petrescu, A. M. R., Davis, S. J., Liu, Z., Grassi, G., Albergel, C., and Chevallier, F.: Comparing national greenhouse gas budgets reported in UNFCCC inventories against atmospheric inversions, *Earth Syst. Sci. Data Discuss.*, 1–59, <https://doi.org/10.5194/essd-2021-235>, 2021.
- Dorfman, R.: A formula for the Gini Coefficient. *The Review of Economics and Statistics* Vol. 61, No. 1, <https://doi.org/10.2307/1924845>, 1979.
- FAOSTAT, available at: <https://www.fao.org/faostat/en/#data/GT>; last access: May 2022, 2022.

1185 Friedlingstein, P., Jones, M. W., O’Sullivan, M., Andrew, R. M., Hauck, J., Peters, G. P., Peters, W., Pongratz,
1186 J., Sitch, S., Le Quéré, C., Bakker, D. C. E., Canadell, J. G., Ciais, P., Jackson, R. B., Anthoni, P., Barbero, L.,
1187 Bastos, A., Bastrikov, V., Becker, M., Bopp, L., Buitenhuis, E., Chandra, N., Chevallier, F., Chini, L. P., Currie,
1188 K. I., Feely, R. A., Gehlen, M., Gilfillan, D., Gkritzalis, T., Goll, D. S., Gruber, N., Gutekunst, S., Harris, I.,
1189 Haverd, V., Houghton, R. A., Hurtt, G., Ilyina, T., Jain, A. K., Joetzjer, E., Kaplan, J. O., Kato, E., Klein
1190 Goldewijk, K., Korsbakken, J. I., Landschützer, P., Lauvset, S. K., Lefèvre, N., Lenton, A., Lienert, S.,
1191 Lombardozzi, D., Marland, G., McGuire, P. C., Melton, J. R., Metzl, N., Munro, D. R., Nabel, J. E. M. S.,
1192 Nakaoka, S.-I., Neill, C., Omar, A. M., Ono, T., Peregón, A., Pierrot, D., Poulter, B., Rehder, G., Resplandy,
1193 L., Robertson, E., Rödenbeck, C., Séférian, R., Schwinger, J., Smith, N., Tans, P. P., Tian, H., Tilbrook, B.,
1194 Tubiello, F. N., van der Werf, G. R., Wiltshire, A. J., and Zaehle, S.: Global Carbon Budget 2019, *Earth Syst.*
1195 *Sci. Data*, 11, 1783–1838, <https://doi.org/10.5194/essd-11-1783-2019>, 2019.

1196
1197 Friedlingstein, P., O’Sullivan, M., Jones, M. W., Andrew, R. M., Hauck, J., Olsen, A., Peters, G. P., Peters,
1198 W., Pongratz, J., Sitch, S., Le Quéré, C., Canadell, J. G., Ciais, P., Jackson, R. B., Alin, S., Aragão, L. E. O.
1199 C., Arneeth, A., Arora, V., Bates, N. R., Becker, M., Benoit-Cattin, A., Bittig, H. C., Bopp, L., Bultan, S.,
1200 Chandra, N., Chevallier, F., Chini, L. P., Evans, W., Florentie, L., Forster, P. M., Gasser, T., Gehlen, M.,
1201 Gilfillan, D., Gkritzalis, T., Gregor, L., Gruber, N., Harris, I., Hartung, K., Haverd, V., Houghton, R. A., Ilyina,
1202 T., Jain, A. K., Joetzjer, E., Kadono, K., Kato, E., Kitidis, V., Korsbakken, J. I., Landschützer, P., Lefèvre, N.,
1203 Lenton, A., Lienert, S., Liu, Z., Lombardozzi, D., Marland, G., Metzl, N., Munro, D. R., Nabel, J. E. M. S.,
1204 Nakaoka, S.-I., Niwa, Y., O’Brien, K., Ono, T., Palmer, P. I., Pierrot, D., Poulter, B., Resplandy, L., Robertson,
1205 E., Rödenbeck, C., Schwinger, J., Séférian, R., Skjelvan, I., Smith, A. J. P., Sutton, A. J., Tanhua, T., Tans, P.
1206 P., Tian, H., Tilbrook, B., van der Werf, G., Vuichard, N., Walker, A. P., Wanninkhof, R., Watson, A. J., Willis,
1207 D., Wiltshire, A. J., Yuan, W., Yue, X., and Zaehle, S.: Global Carbon Budget 2020, *Earth Syst. Sci. Data*, 12,
1208 3269–3340, <https://doi.org/10.5194/essd-12-3269-2020>, 2020.

1209
1210 Gilfillan, D., and Marland G.: CDIAC-FF: global and national CO2 emissions from fossil fuel combustion and
1211 cement manufacture: 1751–2017, <https://doi.org/10.5194/essd-13-1667-2021>, 2021.

1212
1213 Grassi, G., House, J., Kurz, W. A., Cescatti, A., Houghton, R. A., Peters, G. P., Sanz, M. J., Viñas, R. A.,
1214 Alkama, R., Arneeth, A., Bondeau, A., Dentener, F., Fader, M., Federici, S., Friedlingstein, P., Jain, A. K., Kato,
1215 E., Koven, C. D., Lee, D., Nabel, J. E. M. S., Nassikas, A. A., Perugini, L., Rossi, S., Sitch, S., Viovy, N.,
1216 Wiltshire, A., and Zaehle, S.: Reconciling global-model estimates and country reporting of anthropogenic forest
1217 CO2 sinks, *Nat. Clim. Change*, 8, 914–920, <https://doi.org/10.1038/s41558-018-0283-x>, 2018.

1218
1219 Grassi, G., Stehfest, E., Rogelj, J., van Vuuren, D., Cescatti, A., House, J., Nabuurs, G.-J., Rossi, S., Alkama,
1220 R., Viñas, R. A., Calvin, K., Ceccherini, G., Federici, S., Fujimori, S., Gusti, M., Hasegawa, T., Havlik, P.,
1221 Humpenöder, F., Korosuo, A., Perugini, L., Tubiello, F. N., and Popp, A.: Critical adjustment of land mitigation
1222 pathways for assessing countries’ climate progress, *Nat. Clim. Change*, 11, 425–434,
1223 <https://doi.org/10.1038/s41558-021-01033-6>, 2021.

1224
1225 Grassi, G., Conchedda, G., Federici, S., Abad Viñas, R., Korosuo, A., Melo, J., Rossi, S., Sandker, M.,
1226 Somogyi, Z., and Tubiello, F. N.: Carbon fluxes from land 2000–2020: bringing clarity on countries’ reporting,
1227 *Biogeosciences and biodiversity*, <https://doi.org/10.5194/essd-2022-104>, 2022.

1228
1229 Gütschow, J., Jeffery, M. L., Gieseke, R., Gebel, R., Stevens, D., Krapp, M., and Rocha, M.: The PRIMAP-
1230 hist national historical emissions time series, *Earth Syst. Sci. Data*, 8, 571–603, [https://doi.org/10.5194/essd-8-](https://doi.org/10.5194/essd-8-571-2016)
1231 [571-2016](https://doi.org/10.5194/essd-8-571-2016), 2016.

1232

1233 Gütschow, J., Günther, A., Jeffery, M. L., and Gieseke, R.: The PRIMAP-hist national historical emissions
1234 time series (1850-2018) v2.2, <https://doi.org/10.5281/zenodo.4479172>, 2021.

1235

1236 Houghton, R. A., House, J. I., Pongratz, J., van der Werf, G. R., DeFries, R. S., Hansen, M. C., Le Quéré, C.,
1237 and Ramankutty, N.: Carbon emissions from land use and land-cover change, *Biogeosciences*, 9, 5125–5142,
1238 <https://doi.org/10.5194/bg-9-5125-2012>, 2012.

1239

1240 IMF: International Monetary Fund: International Monetary Fund website, available at:
1241 <https://www.imf.org/en/Publications/fandd/issues/Series/Back-to-Basics/gross-domestic-product-GDP>, last
1242 access : February 2022.

1243

1244 IPCC: Good practice guidance for land use, land-use change and forestry /The Intergovernmental Panel on
1245 Climate Change. Edited by: Penman, J., Hayama, Kanagawa, 2006.

1246

1247 IPCC: Climate Change and Land: an IPCC special report on climate change, desertification, land degradation,
1248 sustainable land management, food security, and greenhouse gas fluxes in terrestrial ecosystems, [Shukla, P.R.,
1249 Skea, J., CalvoBuendia, E., Masson-Delmotte, V., Pörtner, H.-O., Roberts, D. C., Zhai, P., Slade, R., Connors,
1250 S., van Diemen, R., Ferrat, M., Haughey, E., Luz, S., Neogi, S., Pathak, M., Petzold, J., Portugal Pereira, J.,
1251 Vyas, P., Huntley, E., Kissick, K., Belkacemi, M., Malley, J. (eds.)]. In press, 2019.

1252

1253 IPCC: Revised 1996 IPCC Guidelines for National Greenhouse Inventories, IPCC/OECD/IEA, Paris, France,
1254 ISBN 92-64-15578- 3, 1997.

1255

1256 IPCC: 2006 IPCC guidelines for National Greenhouse Gas Inventories, IGES, ISBN 4-88788-032-4, 2006.

1257

1258 IPCC: 2019 Refinement to the 2006 IPCC Guidelines for National Greenhouse Gas Inventories, edited by:
1259 Buendia, E., Tanabe, K., Kranjc, A., Baasansuren, J., Fukuda, M., Ngarize, S., Osako, A., Pyrozhenko, Y.,
1260 Shermanau, P., and Federici, S., Intergovernmental Panel on Climate Change (IPCC), Switzerland, ISBN 978-
1261 4-88788-232-4, 2019.

1262

1263 IPCC: Climate Change 2021: The Physical Science Basis. Contribution of Working Group I to the Sixth
1264 Assessment Report of the Intergovernmental Panel on Climate Change [Masson-Delmotte, V., P. Zhai, A.
1265 Pirani, S.L. Connors, C. Péan, S. Berger, N. Caud, Y. Chen, L. Goldfarb, M.I. Gomis, M. Huang, K. Leitzell,
1266 E. Lonnoy, J.B.R. Matthews, T.K. Maycock, T. Waterfield, O. Yelekçi, R. Yu, and B. Zhou (eds.)]. Cambridge
1267 University Press, Cambridge, United Kingdom and New York, NY, USA, In press,
1268 doi:10.1017/9781009157896, 2021.

1269

1270 Janssens-Maenhout, G., Pinty, B., Dowell, M., Zunker, H., Andersson, E., Balsamo, G., Bézy, J.-L., Brunhes,
1271 T., Bösch, H., Bojkov, B., Brunner, D., Buchwitz, M., Crisp, D., Ciais, P., Counet, P., Dee, D., Gon, H. D. van
1272 der, Dolman, H., Drinkwater, M. R., Dubovik, O., Engelen, R., Fehr, T., Fernandez, V., Heimann, M.,
1273 Holmlund, K., Houweling, S., Husband, R., Juvyns, O., Kentarchos, A., Landgraf, J., Lang, R., Löscher, A.,
1274 Marshall, J., Meijer, Y., Nakajima, M., Palmer, P. I., Peylin, P., Rayner, P., Scholze, M., Sierk, B., Tamminen,
1275 J., and Veeffkind, P.: Toward an Operational Anthropogenic CO₂ Emissions Monitoring and Verification
1276 Support Capacity, *Bull. Am. Meteorol. Soc.*, 101, E1439–E1451, <https://doi.org/10.1175/BAMS-D-19-0017.1>,
1277 2020.

1278

1279 van der Laan-Luijkx, I. T., van der Velde, I. R., van der Veen, E., Tsuruta, A., Stanislawski, K.,
1280 Babenhauerheide, A., Zhang, H. F., Liu, Y., He, W., Chen, H., Masarie, K. A., Krol, M. C., and Peters, W.:

1281 The CarbonTracker Data Assimilation Shell (CTDAS) v1.0: implementation and global carbon balance 2001–
1282 2015, *Geosci. Model Dev.*, 10, 2785–2800, <https://doi.org/10.5194/gmd-10-2785-2017>, 2017.
1283
1284 Liousse, C., Assamoi, E., Criqui, P., Granier, C., and Rosset, R.: Explosive growth in African combustion
1285 emissions from 2005 to 2030, *Environ. Res. Lett.*, 9, 035003, <https://doi.org/10.1088/1748-9326/9/3/035003>,
1286 2014.
1287
1288 Mostefaoui, M., Ciais, P., McGrath, M. J., Peylin, P., Prabir, P. K., Saunio, M., Chevallier, F., Sitch, S.,
1289 Rodenbeck, C., Lujikx, I., and Thompson, R.: Datasets for greenhouse gasses emissions and removals from
1290 inventories and global models over Africa v0.1, Zenodo [data set], <https://doi.org/10.5281/zenodo.7347077>,
1291 2022.
1292
1293 Monks, S. A., Arnold, S. R., Hollaway, M. J., Pope, R. J., Wilson, C., Feng, W., Emmerson, K. M., Kerridge,
1294 B. J., Latter, B. L., Miles, G. M., Siddans, R., and Chipperfield, M. P.: The TOMCAT global chemical transport
1295 model v1.6: description of chemical mechanism and model evaluation, *Geosci. Model Dev.*, 10, 3025–3057,
1296 <https://doi.org/10.5194/gmd-10-3025-2017>, 2017.
1297
1298 Nickless, A., Scholes, R. J., Vermeulen, A., Beck, J., López-Ballesteros, A., Ardö, J., Karstens, U., Rigby, M.,
1299 Kasurinen, V., Pantazatou, K., Jorch, V., and Kutsch, W.: Greenhouse gas observation network design for
1300 Africa, *Tellus B Chem. Phys. Meteorol.*, 72, 1–30, <https://doi.org/10.1080/16000889.2020.1824486>, 2020.
1301
1302 Patra, P. K., Takigawa, M., Watanabe, S., Chandra, N., Ishijima, K., and Yamashita, Y.: Improved Chemical
1303 Tracer Simulation by MIROC4.0-based Atmospheric Chemistry-Transport Model (MIROC4-ACTM), *Sola*,
1304 14, 91–96, <https://doi.org/10.2151/sola.2018-016>, 2018.
1305
1306 Perugini, L., Pellis, G., Grassi, G., Ciais, P., Dolman, H., House, J. I., Peters, G. P., Smith, P., Günther, D., and
1307 Peylin, P.: Emerging reporting and verification needs under the Paris Agreement: How can the research
1308 community effectively contribute?, *Environ. Sci. Policy*, 122, 116–126,
1309 <https://doi.org/10.1016/j.envsci.2021.04.012>, 2021.
1310
1311 Petrescu, A. M. R., Qiu, C., Ciais, P., Thompson, R. L., Peylin, P., McGrath, M. J., Solazzo, E., Janssens-
1312 Maenhout, G., Tubiello, F. N., Bergamaschi, P., Brunner, D., Peters, G. P., Höglund-Isaksson, L., Regnier, P.,
1313 Lauerwald, R., Bastviken, D., Tsuruta, A., Winiwarter, W., Patra, P. K., Kuhnert, M., Oreggioni, G. D., Crippa,
1314 M., Saunio, M., Perugini, L., Markkanen, T., Aalto, T., Groot Zwaafink, C. D., Tian, H., Yao, Y., Wilson, C.,
1315 Conchedda, G., Günther, D., Leip, A., Smith, P., Haussaire, J.-M., Leppänen, A., Manning, A. J., McNorton,
1316 J., Brockmann, P., and Dolman, A. J.: The consolidated European synthesis of CH₄ and N₂O emissions for the
1317 European Union and United Kingdom: 1990–2017, *Earth Syst. Sci. Data*, 13, 2307–2362,
1318 <https://doi.org/10.5194/essd-13-2307-2021>, 2021.
1319
1320 Pongratz, J., Reick, C. H., Houghton, R. A., & House, J. I.: Terminology as a key uncertainty in net land use
1321 and land cover change carbon flux estimates. *Earth System Dynamics*, 5(1), 177-195.
1322 <https://doi.org/10.5194/esd-5-177-2014>, 2014.
1323
1324 PRIMAP-hist: PRIMAP-hist dataset, available at: <https://www.pik-potsdam.de/paris-reality-check/primap-hist>
1325 (last access: April 2022), 2021.
1326
1327 Rödenbeck, C.: Estimating CO₂ sources and sinks from atmospheric mixing ratio measurements using a global
1328 inversion of atmospheric transport, undefined, 2005.
1329

1330 Rodgers, C. D.: Inverse Methods For Atmospheric Sounding: Theory And Practice, World Scientific, 256 pp.,
1331 2000.

1332

1333 Saunio, M., Stavert, A. R., Poulter, B., Bousquet, P., Canadell, J. G., Jackson, R. B., Raymond, P. A.,
1334 Dlugokencky, E. J., Houweling, S., Patra, P. K., Ciais, P., Arora, V. K., Bastviken, D., Bergamaschi, P., Blake,
1335 D. R., Brailsford, G., Bruhwiler, L., Carlson, K. M., Carrol, M., Castaldi, S., Chandra, N., Crevoisier, C., Crill,
1336 P. M., Covey, K., Curry, C. L., Etiope, G., Frankenberg, C., Gedney, N., Hegglin, M. I., Höglund-Isaksson, L.,
1337 Hugelius, G., Ishizawa, M., Ito, A., Janssens-Maenhout, G., Jensen, K. M., Joos, F., Kleinen, T., Krummel, P.
1338 B., Langenfelds, R. L., Laruelle, G. G., Liu, L., Machida, T., Maksyutov, S., McDonald, K. C., McNorton, J.,
1339 Miller, P. A., Melton, J. R., Morino, I., Müller, J., Murguia-Flores, F., Naik, V., Niwa, Y., Noce, S., O'Doherty,
1340 S., Parker, R. J., Peng, C., Peng, S., Peters, G. P., Prigent, C., Prinn, R., Ramonet, M., Regnier, P., Riley, W.
1341 J., Rosentreter, J. A., Segers, A., Simpson, I. J., Shi, H., Smith, S. J., Steele, L. P., Thornton, B. F., Tian, H.,
1342 Tohjima, Y., Tubiello, F. N., Tsuruta, A., Viovy, N., Voulgarakis, A., Weber, T. S., van Weele, M., van der
1343 Werf, G. R., Weiss, R. F., Worthy, D., Wunch, D., Yin, Y., Yoshida, Y., Zhang, W., Zhang, Z., Zhao, Y.,
1344 Zheng, B., Zhu, Q., Zhu, Q., and Zhuang, Q.: The Global Methane Budget 2000–2017, *Earth Syst. Sci. Data*,
1345 12, 1561–1623, <https://doi.org/10.5194/essd-12-1561-2020>, 2020.

1346

1347 Schulz, E., Speekenbrink, M., Krause, A.: A tutorial on Gaussian process regression: Modelling, exploring,
1348 and exploiting functions, *Journal of Mathematical Psychology*, <https://doi.org/10.1016/j.jmp.2018.03.001>,
1349 2018.

1350

1351 Sitch, S., Huntingford, C., Gedney, N., Levy, P. E., Lomas, M., Piao, S. L., Betts, R., Ciais, P., Cox, P.,
1352 Friedlingstein, P., Jones, C. D., Prentice, I. C., and Woodward, F. I.: Evaluation of the terrestrial carbon cycle,
1353 future plant geography and climate-carbon cycle feedbacks using five Dynamic Global Vegetation Models
1354 (DGVMS), *Glob. Change Biol.*, 14, 2015–2039, <https://doi.org/10.1111/j.1365-2486.2008.01626.x>, 2008.

1355

1356 Thompson, R. L., Chevallier, F., Crotwell, A. M., Dutton, G., Langenfelds, R. L., Prinn, R. G., Weiss, R. F.,
1357 Tohjima, Y., Nakazawa, T., Krummel, P. B., Steele, L. P., Fraser, P., O'Doherty, S., Ishijima, K., and Aoki,
1358 S.: Nitrous oxide emissions 1999 to 2009 from a global atmospheric inversion, *Atmospheric Chem. Phys.*, 14,
1359 1801–1817, <https://doi.org/10.5194/acp-14-1801-2014>, 2014.

1360

1361 Tian, H., Xu, R., Canadell, J. G., Thompson, R. L., Winiwarter, W., Suntharalingam, P., Davidson, E. A., Ciais,
1362 P., Jackson, R. B., Janssens-Maenhout, G., Prather, M. J., Regnier, P., Pan, N., Pan, S., Peters, G. P., Shi, H.,
1363 Tubiello, F. N., Zaehle, S., Zhou, F., Arneth, A., Battaglia, G., Berthet, S., Bopp, L., Bouwman, A. F.,
1364 Buitenhuis, E. T., Chang, J., Chipperfield, M. P., Dangal, S. R. S., Dlugokencky, E., Elkins, J. W., Eyre, B. D.,
1365 Fu, B., Hall, B., Ito, A., Joos, F., Krummel, P. B., Landolfi, A., Laruelle, G. G., Lauerwald, R., Li, W., Lienert,
1366 S., Maavara, T., MacLeod, M., Millet, D. B., Olin, S., Patra, P. K., Prinn, R. G., Raymond, P. A., Ruiz, D. J.,
1367 van der Werf, G. R., Vuichard, N., Wang, J., Weiss, R. F., Wells, K. C., Wilson, C., Yang, J., and Yao, Y.: A
1368 comprehensive quantification of global nitrous oxide sources and sinks, *Nature*, 586, 248–256,
1369 <https://doi.org/10.1038/s41586-020-2780-0>, 2020.

1370

1371 Tongwane, M. I. and Moeletsi, M. E.: A review of greenhouse gas emissions from the agriculture sector in
1372 Africa, *Agric. Syst.*, 166, 124–134, <https://doi.org/10.1016/j.agsy.2018.08.011>, 2018.

1373 UNFCCC: UNFCCC: National Inventory Submissions, available at: <https://unfccc.int/> (last access : March
1374 2021), 2021.

1375

1376 UNFCCC REDD+: REDD+ National Reports, available at: <https://redd.unfccc.int/submissions.html?topic=6>
1377 (last access: July 2022), 2022.

1378 United Nations Department of Economic and Social Affairs, Population Division: World Population Prospects
1379 2019: Summary of Results, 2019.
1380
1381 Valentini, R., Arneth, A., Bombelli, A., Castaldi, S., Cazzolla Gatti, R., Chevallier, F., Ciais, P., Grieco, E.,
1382 Hartmann, J., Henry, M., Houghton, R. A., Jung, M., Kutsch, W. L., Malhi, Y., Mayorga, E., Merbold, L.,
1383 Murray-Tortarolo, G., Papale, D., Peylin, P., Poulter, B., Raymond, P. A., Santini, M., Sitch, S., Vaglio Laurin,
1384 G., van der Werf, G. R., Williams, C. A., and Scholes, R. J.: A full greenhouse gases budget of Africa: synthesis,
1385 uncertainties, and vulnerabilities, *Biogeosciences*, 11, 381–407, <https://doi.org/10.5194/bg-11-381-2014>, 2014.
1386
1387 van der Werf, G. R., Randerson, J. T., Giglio, L., van Leeuwen, T. T., Chen, Y., Rogers, B. M., Mu, M., van
1388 Marle, M. J. E., Morton, D. C., Collatz, G. J., Yokelson, R. J., and Kasibhatla, P. S.: Global fire emissions
1389 estimates during 1997–2016, *Earth Syst. Sci. Data*, 9, 697–720, <https://doi.org/10.5194/essd-9-697-2017>, 2017.
1390
1391 Wilson, C., Chipperfield, M. P., Gloor, M., and Chevallier, F.: Development of a variational flux inversion
1392 system (INVICAT v1.0) using the TOMCAT chemical transport model, *Geosci. Model Dev.*, 7, 2485–2500,
1393 <https://doi.org/10.5194/gmd-7-2485-2014>, 2014.
1394
1395 World Bank: GDP exchange rate estimates, available at
1396 <https://data.worldbank.org/indicator/NY.GDP.MKTP.CD> last accessed, 2019.
1397
1398 World Bank: World Bank economic data, available at: <https://www.worldbank.org/> (last access: May 2022),
1399 2022.
1400
1401 Zhu, Y., Merbold, L., Pelster, D., Diaz-Pines, E., Wanyama, G. N., and Butterbach-Bahl, K.: Effect of Dung
1402 Quantity and Quality on Greenhouse Gas Fluxes From Tropical Pastures in Kenya, *Glob. Biogeochem. Cycles*,
1403 32, 1589–1604, <https://doi.org/10.1029/2018GB005949>, 2018.
1404
1405 van der Zwaan, B., Kober, T., Longa, F. D., van der Laan, A., and Jan Kramer, G.: An integrated assessment
1406 of pathways for low-carbon development in Africa, *Energy Policy*, 117, 387–395,
1407 <https://doi.org/10.1016/j.enpol.2018.03.017>, 2018.
1408